Dynamic viscoelastic effects on sound wave diffraction by spherical and cylindrical shells submerged in and filled with viscous compressible fluids

Seyyed M. Hasheminejad and Naemeh Safari
Department of Mechanical Engineering, Iran University of Science and Technology, Narmak, Tehran 16844, Iran
Tel.: +9821 73912936; 9821 2557166; Fax: +9821 7451143; E-mail: hashemi@iust.ac.ir

Abstract. An analysis for sound scattering by fluid-filled spherical and cylindrical viscoelastic shells immersed in viscous fluids is outlined. The dynamic viscoelastic properties of the scatterer and the viscosity of the surrounding and core fluids are rigorously taken into account in the solution of the acoustic scattering problem. The novel features of Havriliak-Negami model for viscoelastic material dynamic behaviour description along with the appropriate wave-harmonic field expansions and the pertinent boundary conditions are employed to develop a closed-form solution in form of infinite series. Subsequently, the associated acoustic field quantities such as the scattered far-field pressure directivity pattern, form function amplitude, transmitted intensity ratio, and acoustic force magnitude are evaluated for given sets of medium physical properties. Numerical results clearly indicate that in addition to the traditional fluid viscosity-related mechanisms, the dynamic viscoelastic properties of the shell material as well as its thickness can be of major significance in sound scattering. Limiting cases are examined and fair agreements with well-known solutions are established.

1. Introduction

Historically, sound wave scattering by cylindrical and spherical objects has been investigated quite extensively since works of Rayleigh [1] and Lamb [2]. For example, the scattering of acoustic waves has been broadly studied for a rigid, fixed, solid sphere and circular cylinder [2–4]; for elastic solid sphere and a circular cylinder [5–10]; for elastic spherical and cylindrical shells [11–17], and for coated shells [18–20] in inviscid fluids. On the other hand, investigations of sound scattering by various objects with allowance for various dissipation mechanisms, such as viscous and thermal losses and complicated boundary or scatterer models, have been reported in great many papers [21–25]. The sustained interest in these problems is due to the importance of scattering and attenuation in many areas of research such as cloud physics, rocket propulsion, dispersion ultrasonics and underwater acoustics. The inclusion of viscosity in the fluid model was first made by Sewell [26], who treated sound absorption by rigid, fixed spheres and circular cylinders in a viscous gas. Later, Lamb [2] simplified the Sewell's treatment and studied sound scattering by rigid, fixed or movable spheres in viscous fluid. The most well known acoustic theory for heterogeneous systems was developed by Epstein and Carhart [27], Allegra and Hawley [28] (i.e., the

so called ECAH theory). Lin and Raptis [29,30] presented analytical solutions as well as numerical results for the boundary value problem concerning the interaction of a plane sound wave with (thermo)elastic solid cylinders and spheres immersed in (thermo)viscous fluid. They studied the effects of the fluid viscosity (thermal conductivity), and scatterer's (thermo)elasticity on acoustic-wave scattering patterns and acoustic-radiation force. Later, the same authors presented a general analysis for scattering of a plane sound wave obliquely incident upon a thin, elastic circular rod immersed in an unbounded viscous fluid [31]. The scattered fields of the incident sound wave, the interaction of the sound waves and the rod, and sound radiation by acoustoelastic vibrations of the rod were studied in great details. Likewise, acoustic scattering from a spherical shell including viscous and thermal effects in the surrounding fluid and also the viscoelastic losses in both core and shell material was analyzed in [32]. Hasegawa and Watanabe [33] modified the standard harmonic series theory to study the effect of hysteresis type of absorption on acoustic field of an absorbing sphere immersed in an ideal fluid. Their analysis, however, is applicable to materials with frequency-independent sound absorption per wavelength and may not be considered to be satisfactory from the standpoint of generality and completeness. Just recently, Hasheminejad and Harsini [34] employed the novel features of Havriliak-Negami (HN) model to investigate effects of dynamic viscoelastic properties on acoustic scattering by a solid sphere submerged in a viscous fluid. The prime objective of present work is to utilize HN model to investigate effects of dynamic viscoelastic properties on acoustic interaction of plane sound waves with fluid-filled spherical and cylindrical shells submerged in viscous fluids.

2. Viscoelastic model

Accurate mathematical modelling of viscoelastic materials is difficult mainly because their measured dynamic properties are frequency and temperature dependent, and can also depend on the type of deformation and amplitude. Consequently, mathematical models describing the behaviour of viscoelastic materials cannot be clearly linked to the physical principles involved and thus empirical approaches are used. The most popular approach, called the structural damping model, uses complex constants as the material moduli. Strictly speaking, for viscoelastic and isotropic materials, two independent complex moduli are necessary for mechanical characterization; for example the Young's modulus $E^*(\omega)$ and the shear modulus $G^*(\omega)$. Both moduli, in principle, are frequency dependent. The main difficulty is the simultaneous presence of the Young's and shear complex moduli as well as the Poisson ratio. Practically, however, for viscoelastic isotropic materials the hypothesis of a constant (frequency-independent) and real Poisson ratio is often adopted [35,36]. This assumption has been validated with some experiments [37] revealing that the imaginary part of the Poisson ratio of elastomers is less than 1% of the real part. For elastomers, the Poisson ratio is often supposed to have the constant value 0.5 (i.e., incompressible material), which implies that

$$G^*(\omega) = G'(\omega) + iG''(\omega) = \frac{E^*(\omega)}{2(1+v)} \approx \frac{1}{3}E^*(\omega) \tag{1}$$

Frequency dependence of $G'(\omega)$ and $G''(\omega)$ in the viscoelastic transition region has been the object of many experimental and theoretical studies [38]. The most successful description for the frequency dependence of the complex modulus of polymers in the glass transition region is perhaps given by Havriliak-Negami model [39]. According to HN model, the real and imaginary parts of the complex modulus are given by [40]

$$G'(\omega) = G_\infty + \frac{(G_0 - G_\infty)\cos(\beta\theta)}{[1 + 2\omega^\alpha\tau^\alpha\cos\gamma + \omega^{2\alpha}\tau^{2\alpha}]^{\beta/2}}$$
$$G''(\omega) = \frac{(G_\infty - G_0)\sin(\beta\theta)}{[1 + 2\omega^\alpha\tau^\alpha\cos\gamma + \omega^{2\alpha}\tau^{2\alpha}]^{\beta/2}} \tag{2}$$

where $\gamma = \alpha\pi/2$, and the loss factor is specified by

$$\eta(\omega) = \frac{G''(\omega)}{G'(\omega)} = \frac{(1-\chi)\sin(\beta\theta)}{[1 + 2\omega^\alpha\tau^\alpha\cos\gamma + \omega^{2\alpha}\tau^{2\alpha}]^{\beta/2} - (1-\chi)\cos(\beta\theta)} \tag{3}$$

in which $\chi = G_0/G_\infty$, and

$$\theta(\omega) = \tan^{-1} \frac{\omega^\alpha \tau^\alpha \sin\gamma}{1 + \omega^\alpha \tau^\alpha \cos\gamma} \tag{4}$$

Here we note that $\eta(\omega)$ depends only on the ratio $\chi = G_0/G_\infty$, not on their individual values. Furthermore, G_0 (relaxed modulus) and G_∞ (unrelaxed modulus) are the limiting values of the shear modulus at low and high frequencies, respectively, $\tau (= 1/\omega_0)$ is the relaxation time associated with the polymer glass transition center frequency (loss factor peak), α is a dimensionless parameter $(0 < \alpha < 1)$ that governs the width of the relaxation, and β is another dimensionless parameter $(0 < \beta < 1)$ that governs the asymmetry of the relaxation.

3. Governing field equations

Following the standard methods of continuum mechanics, the linearized equations of continuity and Navier-Stokes for a viscous non-heat-conducting compressible fluid are respectively [41]

$$\begin{aligned} &\frac{\partial \rho}{\partial t} + \rho \nabla \cdot \boldsymbol{u} = 0 \\ &\rho \frac{\partial u}{\partial t} + \nabla p = \mu \nabla^2 \boldsymbol{u} + \left(\frac{1}{3}\mu + \mu_b\right) \nabla(\nabla \cdot \boldsymbol{u}) \end{aligned} \tag{5}$$

Here, ρ is the mass density, and p represents the deviation of pressure from its mean value, $\boldsymbol{u}$ is the fluid velocity vector, and μ and μ_b are the shear and the expansive (bulk) coefficient of viscosity, respectively. For a barotropic fluid, the linearized equation of state is $p = c^2\rho$, where, as usual, c is the ideal speed of sound evaluated at ambient conditions. Equation (5) can readily be combined to yield a single equation for the velocity vector $\boldsymbol{u}$:

$$\frac{\partial^2 \boldsymbol{u}}{\partial t^2} - c^2 \nabla(\nabla \cdot \boldsymbol{u}) = \frac{\mu}{\rho} \nabla^2 \frac{\partial \boldsymbol{u}}{\partial t} + \frac{1}{\rho}\left(\frac{1}{3}\mu + \mu_b\right) \nabla\left(\nabla \cdot \frac{\partial \boldsymbol{u}}{\partial t}\right) \tag{6}$$

Helmholtz decomposition theorem allows us to resolve the velocity fields as superposition of longitudinal and transverse vector components

$$\boldsymbol{u} = -\nabla\varphi + \nabla \times \boldsymbol{\psi} \tag{7}$$

Introducing the above decomposition into Eq. (6), making use of problem symmetry, $\boldsymbol{\psi} = (0., 0., \psi)$, and the calibration condition, $\nabla \cdot \boldsymbol{\psi} = 0$, a set of two equations is deduced

$$\frac{\partial^2 \varphi}{\partial t^2} = \left[c^2 + \frac{1}{\rho}\left(\frac{4}{3}\mu + \mu_b\right) \frac{\partial}{\partial t}\right] \nabla^2 \varphi, \quad \frac{\partial \psi}{\partial t} = \frac{\mu}{\rho} \nabla^2 \psi \tag{8}$$

Now, since the incident wave is assumed to be monochromatic, with frequency ω, we expect solutions of the form

$$\varphi(r, \theta, t) = Re[\varphi(r, \theta, \omega)e^{-i\omega t}], \quad \psi(r, \theta, t) = Re[\psi(r, \theta, \omega)e^{-i\omega t}] \tag{9}$$

where Re indicates the real part of a complex number, and quantities $\varphi(r, \theta, \omega)$ and $\psi(r, \theta, \omega)$ may be complex. Incorporation of above assumptions in Eq. (8), after some manipulations, yields

$$(\nabla^2 + k_c^2)\varphi = 0, \quad (\nabla^2 + k_s^2)\psi = 0 \tag{10}$$

where the complex compressional and shear wave numbers in the viscous fluid are given by [41]

$$k_c = \frac{\omega}{c}\left(1 + i\frac{\omega\mu}{2\rho c^2}\left(\frac{4}{3} + \frac{\mu_b}{\mu}\right)\right), \quad k_s = (1+i)\sqrt{\frac{\omega\rho}{2\mu}} \tag{11}$$

The viscoelastic material under consideration is assumed to be linear, macroscopically homogeneous, and isotropic for which the constitutive equation, for harmonic time functions, may be written as [42]

$$\sigma_{ij} = \lambda^*(\omega)\delta_{ij}\varepsilon_{kk} + 2\mu_s^*(\omega)\varepsilon_{ij} \tag{12}$$

where δ_{ij} is Kronecker delta symbol, $\lambda^*(\omega)$ and $\mu_s^*(\omega)$ are complex, frequency dependent Lame functions which are determined according to the standard relations
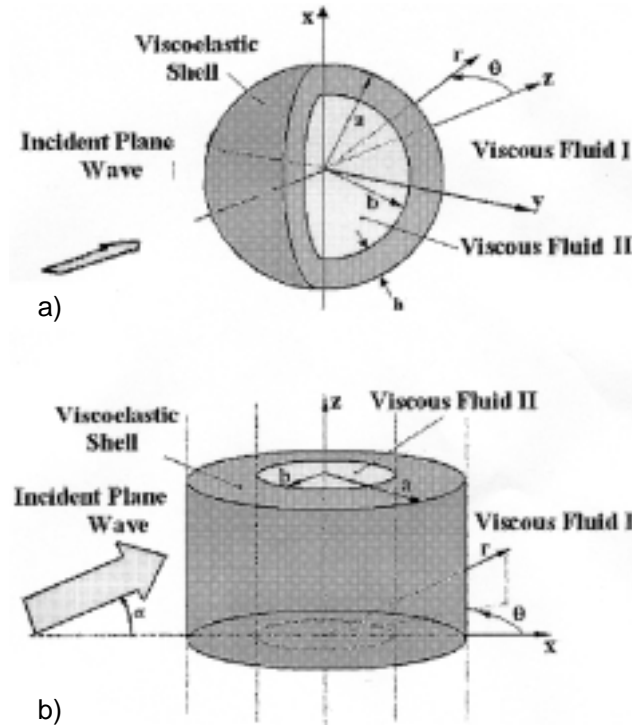
Fig. 1. Problem geometry; a) Spherical coordinate system, b) Cylindrical coordinate system.

$$\lambda^*(\omega) = \frac{2v}{1-2v}G^*(\omega), \quad \mu_s^*(\omega) = G^*(\omega) \tag{13}$$

in which the real and imaginary parts of the complex shear modulus, $G^*(\omega)$, are specified in Eq. (2). The wave motion in the viscoelastic shell is governed by the classical Navier's equation [43]

$$\rho_s \frac{\partial^2 U}{\partial t^2} = \mu_s^* \nabla^2 U + (\lambda^* + \mu_s^*)\nabla(\nabla \cdot U) \tag{14}$$

subject to the appropriate boundary conditions. Here, ρ_s is the solid material density, and U is the vector displacement that can advantageously be expressed as sum of the gradient of a scalar potential and the curl of a vector potential:

$$U = \nabla\Phi + \nabla \times \Psi \tag{15}$$

with the condition $\nabla \cdot \Psi = 0$, and $\Psi = (0., 0., \Psi)$. The above decomposition enables us to separate the dynamic equation of motion into the classical Helmholtz equations:

$$(\nabla^2 + K_c^{*2})\Phi = 0, \quad (\nabla^2 + K_s^{*2})\Psi = 0 \tag{16}$$

where K_c^* and K_s^* are complex wave numbers, known as [42]

$$K_c^* = \frac{\omega}{\sqrt{\frac{\lambda^*(\omega)+2\mu_s^*(\omega)}{\rho_s}}}, \quad K_s^* = \frac{\omega}{\sqrt{\frac{\mu_s^*(\omega)}{\rho_s}}} \tag{17}$$

4. Sound wave diffraction by a spherical viscoelastic shell

In this section we consider the general problem of acoustic scattering from a (viscous) fluid-filled spherical viscoelastic shell suspended in an unbounded viscous fluid. The geometry and the coordinate system used are depicted in Fig. 1a. Mathematically, the dynamics of the problem may be expressed in terms of appropriate scalar

potentials. The expansion of the incident plane wave in spherical coordinate has the form [44]

$$\varphi_{inc.}(r.\theta) = P_0 \sum_{n=0}^{\infty} (2n+1)i^n j_n(k_{c1}r)P_n(\cos\theta) \tag{18}$$

where j_n are spherical Bessel functions [45], P_n are Legendre polynomials, and P_0 is the amplitude of the incident wave. Likewise, keeping in mind the radiation condition, the solutions of the Helmholtz equations for the potentials in the surrounding fluid medium I and the encapsulated fluid medium II can be expressed as a linear combination of outgoing spherical waves as follows

$$\varphi_1(r,\theta) = \sum_{n=0}^{\infty} (2n+1)i^n A_n h_n^{(1)}(k_{c1}r)P_n(\cos\theta), \quad \varphi_2(r,\theta) = \sum_{n=0}^{\infty} (2n+1)i^n G_n j_n(k_{c2}r)P_n(\cos\theta),$$

$$\psi_1(r,\theta) = \sum_{n=1}^{\infty} (2n+1)i^n B_n h_n^{(1)}(k_{s1}r)P_n^1(\cos\theta), \quad \psi_2(r,\theta) = \sum_{n=1}^{\infty} (2n+1)i^n Q_n j_n(k_{s2}r)P_n^1(\cos\theta), \tag{19}$$

where $h_n^{(1)}$ are spherical Hankel functions of first kind [45], $P_n^1 = -(d/d\theta)P_n$ are associated Legendre functions, A_n, B_n, G_n and Q_n are unknown scattering coefficients, and the subscripts 1 and 2 refer to the surrounding fluid medium I and the inner fluid medium II, respectively. Furthermore, the transmitted longitudinal and transverse waves in the viscoelastic shell are represented by

$$\Phi(r,\theta) = \sum_{n=0}^{\infty} (2n+1)i^n [C_n h_n^{(1)}(K_c^*r) + D_n h_n^{(2)}(K_c^*r)]P_n(\cos\theta)$$

$$\Psi(r,\theta) = \sum_{n=1}^{\infty} (2n+1)i^n [E_n h_n^{(1)}(K_s^*r) + F_n h_n^{(2)}(K_s^*r)]P_n^1(\cos\theta) \tag{20}$$

where $h_n^{(2)}$ are spherical Hankel functions of second kind [45] and the superscript * indicates that complex, frequency-dependent viscoelastic properties are involved.

Now considering the basic field equations in spherical coordinates, the velocity components of the waves in r- and θ-directions in terms of potentials in the viscous fluids are [41]

$$u_r^1 = -\frac{\partial\varphi}{\partial r} + \frac{1}{r\sin\theta}\frac{\partial(\psi_1\sin\theta)}{\partial\theta} \quad u_r^2 = -\frac{\partial\varphi_2}{\partial r} + \frac{1}{r\sin\theta}\frac{\partial(\psi_2\sin\theta)}{\partial\theta}$$

$$u_\theta^1 = -\frac{1}{r}\frac{\partial\varphi}{\partial\theta} - \frac{1}{r}\frac{\partial(r\psi_1)}{\partial r} \quad u_\theta^2 = -\frac{1}{r}\frac{\partial\varphi_2}{\partial\theta} - \frac{1}{r}\frac{\partial(r\psi_2)}{\partial r} \tag{21}$$

where $\varphi = \varphi_{inc.} + \varphi_1$. Similarly, the displacement components in the viscoelastic shell are [43]

$$U_r = \frac{\partial\Phi}{\partial r} + \frac{1}{r\sin\theta}\frac{\partial(\Psi\sin\theta)}{\partial\theta} \quad U_\theta = \frac{1}{r}\frac{\partial\Phi}{\partial\theta} - \frac{1}{r}\frac{\partial(r\Psi)}{\partial r} \tag{22}$$

The stress components in the viscous fluids are [41]

$$\sigma_{rr}^1 = -p_1 + \left(\mu_{b1} - \frac{2}{3}\mu_1\right)\Delta_1 + 2\mu_1(\partial u_r^1/\partial r) \quad \sigma_{rr}^2 = -p_2 + \left(\mu_{b2} - \frac{2}{3}\mu_2\right)\Delta_2 + 2\mu_2(\partial u_r^2/\partial r)$$

$$\sigma_{r\theta}^1 = \mu_1\left(\frac{1}{r}\frac{\partial u_r^1}{\partial\theta} + \frac{\partial u_\theta^1}{\partial r} - \frac{u_\theta^1}{r}\right) \quad \sigma_{r\theta}^2 = \mu_2\left(\frac{1}{r}\frac{\partial u_r^2}{\partial\theta} + \frac{\partial u_\theta^2}{\partial r} - \frac{u_\theta^2}{r}\right) \tag{23}$$

where

$$p_1 = -i\omega\rho_1\varphi + \left(\mu_{b1} + \frac{4}{3}\mu_1\right)\Delta_1 \quad p_2 = -i\omega\rho_2\varphi_2 + \left(\mu_{b2} + \frac{4}{3}\mu_2\right)\Delta_2 \tag{24}$$

in which $\Delta_1 = \nabla \cdot \boldsymbol{u}_1 = -\nabla^2\varphi = k_{c1}^2\varphi$, $\Delta_2 = \nabla \cdot \boldsymbol{u}_2 = -\nabla^2\varphi_2 = k_{c2}^2\varphi_2$. Likewise, the stresses in the viscoelastic scatterer are [42]

$$\sigma_{rr}^s = 2\mu_s^* \frac{\partial U_r}{\partial r} + \lambda^* \varepsilon \quad \sigma_{r\theta}^s = \mu_s^* \left(\frac{1}{r} \frac{\partial U_r}{\partial \theta} + \frac{\partial U_\theta}{\partial r} - \frac{U_\theta}{r} \right) \tag{25}$$

where $\varepsilon = \nabla \cdot U = \nabla^2 \Phi = 0 - K_C^{*2} \Phi$.

The appropriate boundary conditions that must hold at the interfaces of the inner and outer fluids with the shell are continuity of velocity and stress components, i.e.,

$$
\begin{aligned}
u_r^1(a,\theta,\omega) &= -i\omega U_r(a,\theta,\omega) & -i\omega U_r(b,\theta,\omega) &= u_r^2(b,\theta,\omega) \\
u_\theta^1(a,\theta,\omega) &= -i\omega U_\theta(a,\theta,\omega) & -i\omega U_\theta(b,\theta,\omega) &= u_\theta^2(b,\theta,\omega) \\
\sigma_{rr}^1(a,\theta,\omega) &= \sigma_{rr}^s(a,\theta,\omega) & \sigma_{rr}^s(b,\theta,\omega) &= \sigma_{rr}^2(b,\theta,\omega) \\
\sigma_{r\theta}^1(a,\theta,\omega) &= \sigma_{r\theta}^s(a,\theta,\omega) & \sigma_{r\theta}^s(b,\theta,\omega) &= \sigma_{r\theta}^2(b,\theta,\omega)
\end{aligned}
\tag{26}
$$

The unknown scattering coefficients shall be determined by imposing the stated boundary conditions. Employing expansions Eqs (18) through (20) in the field Eqs (21) through (25), and substituting the obtained results into the boundary conditions Eq. (26), we obtain, for the n-th mode

$$
\begin{aligned}
&-k_{c1} A_n h_n^{(1)'}(k_{c1}a) + \frac{n(n+1)}{a} B_n h_n^{(1)}(k_{s1}a) + i\omega K_c^* \left[C_n h_n^{(1)'}(K_c^*a) + D_n h_n^{(2)'}(K_c^*a) \right] \\
&+ i\omega \frac{n(n+1)}{a} \left[E_n h_n^{(1)}(K_s^*a) + F_n h_n^{(2)}(K_s^*a) \right] = k_{c1} P_0 j_n'(k_{c1}a)
\end{aligned}
\tag{27a}
$$

$$
\begin{aligned}
&A_n h_n^{(1)}(k_{c1}a) - \left[h_n^{(1)}(k_{s1}a) + k_{s1} a h_n^{(1)'}(k_{s1}a) \right] B_n - i\omega \left[C_n h_n^{(1)}(K_c^*a) + D_n h_n^{(2)}(K_c^*a) \right] \\
&- i\omega \left\{ \left[h_n^{(1)}(K_s^*a) + k_s^* a h_n^{(1)'}(K_s^*a) \right] E_n + \left[h_n^{(2)}(K_s^*a) + K_s^* a h_n^{(2)'}(K_s^*a) \right] F_n \right\} = -P_0 j_n(k_{c1}a)
\end{aligned}
\tag{27b}
$$

$$
\begin{aligned}
&\left[(i\omega\rho_1 - 2\mu_1 k_{c1}^2) h_n^{(1)}(k_{c1}a) - 2\mu_1 k_{c1}^2 h_n^{(1)''}(k_{c1}a) \right] A_n \\
&- \frac{2\mu_1 n(n+1)}{a^2} \left[h_n^{(1)}(k_{s1}a) - k_{s1} a h_n^{(1)'}(k_{s1}a) \right] B_n \\
&- K_c^{*2} \left\{ \left[2\mu_s^* h_n^{(1)''}(K_c^*a) - \lambda^* h_n^{(1)}(K_c^*a) \right] C_n + \left[2\mu_s^* h_n^{(2)''}(K_c^*a) - \lambda^* h_n^{(2)}(K_c^*a) \right] D_n \right\} \\
&+ \frac{2\mu_s^* n(n+1)}{a^2} \left\{ \left[h_n^{(1)}(K_s^*a) - K_s^* a h_n^{(1)'}(K_s^*a) \right] E_n + \left[h_n^{(2)}(K_s^*a) - K_s^* a h_n^{(2)'}(K_s^*a) \right] F_n \right\} \\
&= - \left[(i\omega\rho_1 - 2\mu_1 k_{c1}^2) j_n(k_{c1}a) - 2\mu_1 k_{c1}^2 j_n''(k_{c1}a) \right] P_0
\end{aligned}
\tag{27c}
$$

$$
\begin{aligned}
&-2\mu_1 \left\{ h_n^{(1)}(k_{c1}a) - k_{c1} a h_n^{(1)'}(k_{c1}a) \right\} A_n + \mu_1 \left\{ [2 - n(n+1)] h_n^{(1)}(k_{s1}a) - k_{s1}^2 a^2 h_n^{(1)''}(k_{s1}a) \right\} B_n \\
&+ 2\mu_s^* \left\{ \left\{ K_c^* a h_n^{(1)'}(K_c^*a) - h_n^{(1)}(K_c^*a) \right] C_n + \left\{ K_c^* a h_n^{(2)'}(K_c^*a) - h_n^{(2)}(K_c^*a) \right] D_n \right\} \\
&- \mu_s^* \left\{ [2 - n(n+1)] h_n^{(1)}(K_s^*a) - K_s^{*2} a^2 h_n^{(1)''}(K_s^*a) \right\} E_n \\
&- \mu_s^* \left\{ [2 - n(n+1)] h_n^{(2)}(K_s^*a) - K_s^{*2} a^2 h_n^{(2)''}(K_s^*a) \right\} F_n \\
&= 2\mu_1 \left[j_n(k_{c1}a) - k_{c1} a j_n'(k_{c1}a) \right] P_0
\end{aligned}
\tag{27d}
$$

$$
\begin{aligned}
&i\omega K_c^* \left[C_n h_n^{(1)'}(K_c^*b) + D_n h_n^{(2)'}(K_c^*b) \right] + i\omega \frac{n(n+1)}{b} \left[E_n h_n^{(1)}(K_s^*b) + F_n h_n^{(2)}(K_s^*b) \right] \\
&- k_{c2} G_n j_n'(k_{c2}b) + \frac{n(n+1)}{b} Q_n j_n(k_{c2}b) = 0
\end{aligned}
\tag{27e}
$$

$$-i\omega \left[C_n h_n^{(1)}(K_c^* b) + D_n h_n^{(2)}(K_c^* b)\right] - i\omega \left[h_n^{(1)}(K_s^* b) + K_s^* b h_n^{(1)'}(K_s^* b)\right] E_n$$

$$-i\omega \left[h_n^{(2)}(K_s^* b) + K_s^* b h_n^{(2)'}(K_s^* b)\right] F_n + G_n j_n(k_{c2} b) - \left[j_n(k_{s2} b) + k_{s2} b j_n'(k_{s2} b)\right] Q_n = 0 \tag{27f}$$

$$K_c^{*2} \left\{ \left[\lambda^* h_n^{(1)}(K_c^* b) - 2\mu_s^* h_n^{(1)''}(K_c^* b)\right] C_n + \left[\lambda^* h_n^{(2)}(K_c^* b) - 2\mu_s^* h_n^{(2)''}(K_c^* b)\right] D_n \right\}$$

$$-\frac{2n(n+1)}{b^2}\mu_s^* \left\{ \left[-h_n^{(1)}(K_s^* b) + K_s^* b h_n^{(1)'}(K_s^* b)\right] E_n + \left[-h_n^{(2)}(K_s^* b) + K_s^* b h_n^{(2)'}(K_s^* b)\right] F_n \right\} \tag{27g}$$

$$+ \left[(i\omega\rho_2 - 2\mu_2 k_{c2}^2) j_n(k_{c2} b) - 2\mu_2 k_{c2}^2 j_n''(k_{c2} b)\right] G_n - \frac{2\mu_2 n(n+1)}{b^2} \left[j_n(k_{s2} b) - k_{s2} b j_n'(k_{s2} b)\right] Q_n = 0$$

$$2\mu_s^* \left[K_c^* b h_n^{(1)'}(K_c^* b) - h_n^{(1)}(K_c^* b)\right] C_n + 2\mu_s^* \left[K_c^* b h_n^{(2)'}(K_c^* b) - h_n^{(2)}(K_c^* b)\right] D_n$$

$$-\mu_s^* \left\{ [2 - n(n+1)] h_n^{(1)}(K_s^* b) - K_s^{*2} b^2 h_n^{(1)''}(K_s^* b) \right\} E_n$$

$$-\mu_s^* \left\{ [2 - n(n+1)] h_n^{(2)}(K_s^* b) - K_s^{*2} b^2 h_n^{(2)''}(K_s^* b) \right\} F_n \tag{27h}$$

$$-2\mu_2 \left[j_n(k_{c2} b) - k_{c2} b j_n'(k_{c2} b)\right] G_n + \mu_2 \left\{ [2 - n(n+1)] j_n(k_{s2} b) - \mu_2 k_{s2}^2 b^2 j_n''(k_{s2} b) \right\} Q_n = 0$$

where $n = 0, 1, 2, \ldots$, except for Eqs (27b), (27d), (27f), (27h) where $n = 1, 2, \ldots$

The most relevant acoustic field quantities are scattered pressure and transmitted intensity. Substitution of first of Eq. (19) into the first of Eq. (24) yields the acoustic pressure for harmonic scattered waves. The radial component of the acoustic power flux vector (acoustic intensity) transmitted into the encapsulated fluid medium II may be obtained from [21]

$$I_{trans.}(r, \theta, \omega) = \frac{1}{2} Re \left\{ \sigma_{rr}^2 \times conj(u_r^2) + \sigma_{r\theta}^2 \times conj(u_\theta^2) \right\} \tag{28}$$

where $conj$ stands for the complex conjugate operator. Correspondingly, the quotient $|I_{trans.}/I_{inc.}|$ represents the power transmitted per unit solid angle and per unit incident intensity ($I_{inc.} = P_0 \rho \omega^2 / 2c$) into the shell.

The force acting on the spherical shell due to the acoustic field present in the surrounding viscous fluid medium can be found by determining the fluid stresses on the outer surface of the shell. This force will have only one component that is given by [41]

$$F = 2\pi a^2 \int_0^\pi (\sigma_{rr}^1 \cos\theta - \sigma_{r\theta}^1 \sin\theta) \sin\theta d\theta \tag{29}$$

The fluid stress tensor components as obtained from Eq. (23) may be expressed in the form

$$\sigma_{rr}^1 = \sum_{n=0}^\infty \sigma_{rrn}^1 P_n(\cos\theta) \quad \sigma_{r\theta}^1 = \sum_{n=1}^\infty \sigma_{r\theta n}^1 P_n^1(\cos\theta) \tag{30}$$

Substituting the above expansions into the force Eq. (29), using the appropriate orthogonality relation for Legendre functions [45] and performing the integration, we find

$$F = 2\pi a^2 \left(\frac{2}{3}\sigma_{rr1}^1 + \frac{4}{3}\sigma_{r\theta 1}^1\right) \tag{31}$$

5. Sound wave diffraction by a cylindrical viscoelastic shell

In this section we consider a compressional planar monochromatic sound wave of angular frequency ω obliquely incident upon a (viscous) fluid-filled cylindrical viscoelastic shell immersed in an unbounded viscous fluid at rest (Fig. 1b). When the sound wave meets the shell, both the wave and the obstacle are affected by the interaction.

Consequently, flexural and compressional oscillations in the shell are induced which in turn radiate sound waves into the neighbouring fluid medium and affect the scattered waves. The dynamics of the problem can be expressed in terms of appropriate scalar potentials. The expansion of the incident plane wave in cylindrical coordinate has the form [44]

$$\varphi_{inc.} = P_0 \sum_{n=0}^{\infty} \varepsilon_n i^n J_n(\gamma_{c1}r) \cos n\theta e^{ik_z z} \tag{32}$$

where $\varepsilon_0 = 1$ and $\varepsilon_n = 2$ for $n > 0$, P_0 is the amplitude of the incident wave, J_n are cylindrical Bessel functions of first kind [45], and $\gamma_{c1} = \sqrt{k_{c1}^2 - k_z^2}$ in which $k_z = Re(k_{c1}\sin\alpha)$. Next, noting that the outer fluid medium is unbounded and keeping in mind the radiation condition, the solutions of the Helmholtz equations for the potentials in the surrounding fluid medium I can be expressed as a linear combination of outgoing cylindrical waves as follows

$$\varphi^1 = \sum_{n=0}^{\infty} A_n H_n^{(1)}(\gamma_{c1}r) \cos n\theta e^{ik_z z} \quad \psi_\theta^1 = -\sum_{n=0}^{\infty} B_n H_{n+1}^{(1)}(\gamma_{s1}r) \cos n\theta e^{ik_z z}$$

$$\psi_r^1 = \sum_{n=1}^{\infty} B_n H_{n+1}^{(1)}(\gamma_{s1}r) \sin n\theta e^{ik_z z} \quad \psi_z^1 = \sum_{n=1}^{\infty} C_n H_n^{(1)}(\gamma_{s1}r) \sin n\theta e^{ik_z z} \tag{33}$$

where $H_n^{(1)}$ are cylindrical Hankel functions of first kind [45], A_n, B_n and C_n are unknown scattering coefficients, and $\gamma_{s1} = \sqrt{k_{s1}^2 - k_z^2}$. Furthermore, the velocity potentials in the encapsulated fluid medium II can be expressed as

$$\varphi^2 = \sum_{n=0}^{\infty} M_n J_n(\gamma_{c2}r) \cos n\theta e^{ik_z z} \quad \psi_\theta^2 = -\sum_{n=0}^{\infty} N_n J_{n+1}(\gamma_{s2}r) \cos n\theta e^{ik_z z}$$

$$\psi_r^2 = \sum_{n=1}^{\infty} N_n J_{n+1}(\gamma_{s2}r) \sin n\theta e^{ik_z z} \quad \psi_z^2 = \sum_{n=1}^{\infty} Q_n J_n(\gamma_{s2}r) \sin n\theta e^{ik_z z} \tag{34}$$

where M_n, N_n and Q_n are unknown refraction coefficients, $\gamma_{c2} = \sqrt{k_{c2}^2 - k_z^2}$ and $\gamma_{s2} = \sqrt{k_{s2}^2 - k_z^2}$. Similarly, the transmitted longitudinal and transverse waves in the viscoelastic shell medium are represented by

$$\Phi = \sum_{n=0}^{\infty} \left[D_n H_n^{(1)}(\Gamma_c r) + E_n H_n^{(2)}(\Gamma_c r) \right] \cos n\theta e^{ik_z z}$$

$$\Psi_r = \sum_{n=1}^{\infty} \left[F_n H_{n+1}^{(1)}(\Gamma_s r) + G_n H_{n+1}^{(2)}(\Gamma_s r) \right] \sin n\theta e^{ik_z z}$$

$$\Psi_\theta = -\sum_{n=0}^{\infty} \left[F_n H_{n+1}^{(1)}(\Gamma_s r) + G_n H_{n+1}^{(2)}(\Gamma_s r) \right] \cos n\theta e^{ik_z z} \tag{35}$$

$$\Psi_z = \sum_{n=1}^{\infty} \left[K_n H_n^{(1)}(\Gamma_s r) + L_n H_n^{(2)}(\Gamma_s r) \right] \sin n\theta e^{ik_z z}$$

where $H_n^{(2)}$ are cylindrical Hankel functions of second kind [45], D_n through L_n are unknown transmission coefficients and $\Gamma_c = \sqrt{K_c^{*2} - k_z^2}$, $\Gamma_s = \sqrt{K_s^{*2} - k_z^2}$.

Now considering the basic field equations in cylindrical coordinates, the velocity components of the waves in r- and θ-directions in terms of potentials in the viscous fluids are [29]

$$u_r^1 = -\frac{\partial \varphi}{\partial r} + \frac{1}{r}\frac{\partial \psi_z^1}{\partial \theta} - \frac{\partial \psi_\theta^1}{\partial z} \quad u_r^2 = -\frac{\partial \varphi^2}{\partial r} + \frac{1}{r}\frac{\partial \psi_z^2}{\partial \theta} - \frac{\partial \psi_\theta^2}{\partial z}$$

$$u_\theta^1 = -\frac{1}{r}\frac{\partial \varphi}{\partial \theta} + \frac{\partial \psi_r^1}{\partial z} - \frac{\partial \psi_z^1}{\partial r} \quad u_\theta^2 = -\frac{1}{r}\frac{\partial \varphi^2}{\partial \theta} + \frac{\partial \psi_r^2}{\partial z} - \frac{\partial \psi_z^2}{\partial r} \tag{36}$$

$$u_z^1 = -\frac{\partial \varphi}{\partial z} + \frac{1}{r}\frac{\partial (r\psi_\theta^1)}{\partial r} - \frac{1}{r}\frac{\partial \psi_r^1}{\partial \theta} \quad u_z^2 = -\frac{\partial \varphi^2}{\partial z} + \frac{1}{r}\frac{\partial (r\psi_\theta^2)}{\partial r} - \frac{1}{r}\frac{\partial \psi_r^2}{\partial \theta}$$

where $\varphi = \varphi_{inc.} + \varphi^1$. Similarly, the relevant displacements in the viscoelastic shell are [43]

$$U_r = \frac{\partial \Phi}{\partial r} + \frac{1}{r}\frac{\partial \Psi_z}{\partial \theta} - \frac{\partial \Psi_\theta}{\partial z}$$

$$U_\theta = \frac{1}{r}\frac{\partial \Phi}{\partial \theta} + \frac{\partial \Psi_r}{\partial z} - \frac{\partial \Psi_z}{\partial r} \tag{37}$$

$$U_z = \frac{\partial \Phi}{\partial z} + \frac{1}{r}\frac{\partial (r\Psi_\theta)}{\partial r} - \frac{1}{r}\frac{\partial \Psi_r}{\partial \theta}$$

The stress components in the viscous fluids are [29,31]

$$\sigma_{rr}^1 = -p_1 + (\mu_{b1} - 2\mu_1/3)\Delta_1 + 2\mu_1(\partial u_r^1/\partial r) \quad \sigma_{rr}^1 = -p_2 + (\mu_{b2} - 2\mu_2/3)\,\Delta_2 + 2\mu_2(\partial u_r^2/\partial r)$$

$$\sigma_{r\theta}^1 = \mu_1 \left(\frac{1}{r}\frac{\partial u_r^1}{\partial \theta} + \frac{\partial u_\theta^1}{\partial r} - \frac{u_\theta^1}{r} \right) \quad \sigma_{r\theta}^2 = \mu_2 \left(\frac{1}{r}\frac{\partial u_r^2}{\partial \theta} + \frac{\partial u_\theta^2}{\partial r} - \frac{u_\theta^2}{r} \right) \tag{38}$$

$$\sigma_{rz}^1 = \mu_1 \left(\frac{\partial u_r^1}{\partial z} + \frac{\partial u_z^1}{\partial r} \right) \quad \sigma_{rz}^2 = \mu_2 \left(\frac{\partial u_r^2}{\partial z} + \frac{\partial u_z^2}{\partial r} \right)$$

and the corresponding stresses in the viscoelastic shell are [43]

$$\sigma_{rr}^s = 2\mu_s^* \frac{\partial U_r}{\partial r} + \lambda_s^* \varepsilon$$

$$\sigma_{r\theta}^s = \mu_s^* \left(\frac{1}{r}\frac{\partial U_r}{\partial \theta} + \frac{\partial U_\theta}{\partial r} - \frac{U_\theta}{r} \right) \tag{39}$$

$$\sigma_{rz}^s = \mu_s^* \left(\frac{\partial U_r}{\partial z} + \frac{\partial U_z}{\partial r} \right)$$

where $\varepsilon = \nabla \cdot U = \nabla^2 \Phi = -K_c^{*2}\Phi$.

The appropriate boundary conditions that must hold at the fluid/solid interfaces are simply continuity of velocities and stresses that are written as

$$
\begin{aligned}
u_r^1(a,\theta,\omega) &= -i\omega U_r(a,\theta,\omega) & -i\omega U_r(b,\theta,\omega) &= u_r^2(b,\theta,\omega) \\
u_\theta^1(a,\theta,\omega) &= -i\omega U_\theta(a,\theta,\omega) & -i\omega U_\theta(b,\theta,\omega) &= u_\theta^2(b,\theta,\omega) \\
u_z^1(a,\theta,\omega) &= -i\omega U_z(a,\theta,\omega) & -i\omega U_z(b,\theta,\omega) &= u_z^2(b,\theta,\omega) \\
\sigma_{rr}^1(a,\theta,\omega) &= \sigma_{rr}^s(a,\theta,\omega) & \sigma_{rr}^s(b,\theta,\omega) &= \sigma_{rr}^2(b,\theta,\omega) \\
\sigma_{r\theta}^1(a,\theta,\omega) &= \sigma_{r\theta}^s(a,\theta,\omega) & \sigma_{r\theta}^s(b,\theta,\omega) &= \sigma_{r\theta}^2(b,\theta,\omega) \\
\sigma_{rz}^1(a,\theta,\omega) &= \sigma_{rz}^s(a,\theta,\omega) & \sigma_{rz}^s(b,\theta,\omega) &= \sigma_{rz}^2(b,\theta,\omega)
\end{aligned}
\tag{40}
$$

At this point the unknown scattering coefficients shall be determined by imposing the stated boundary conditions. Employing expansions (32) through (35) in the field Eqs (36) through (39), and substituting obtained results into the boundary conditions Eq. (40), we obtain, for the n-th mode

$$-\gamma_{c1}A_n H_n^{(1)'}(\gamma_{c1}a) + ik_z B_n H_{n+1}^{(1)}(\gamma_{s1}a) + \frac{n}{a}C_n H_n^{(1)}(\gamma_{s1}a)$$

$$+i\omega\Gamma_c \left[D_n H_n^{(1)'}(\Gamma_c a) + E_n H_n^{(2)'}(\Gamma_c a) \right] - \omega k_z \left[F_n H_{n+1}^{(1)}(\Gamma_s a) + G_n H_{n+1}^{(2)}(\Gamma_s a) \right] \tag{41a}$$

$$+i\omega\frac{n}{a} \left[K_n H_n^{(1)}(\Gamma_s a) + L_n H_n^{(2)}(\Gamma_s a) \right] = P_0\varepsilon_n i^n \gamma_{c1}J_n'(\gamma_{c1}a)$$

$$\frac{n}{a}A_n H_n^{(1)}(\gamma_{c1}a) + ik_z B_n H_{n+1}^{(1)}(\gamma_{s1}a) - \gamma_{s1}C_n H_n^{(1)'}(\gamma_{s1}a)$$

$$-i\omega\frac{n}{a} \left[D_n H_n^{(1)}(\Gamma_c a) + E_n H_n^{(2)}(\Gamma_c a) \right] - \omega k_z \left[F_n H_{n+1}^{(1)}(\Gamma_s a) + G_n H_{n+1}^{(2)}(\Gamma_s a) \right] \tag{41b}$$

$$-i\omega\Gamma_s \left[K_n H_n^{(1)'}(\Gamma_s a) + L_n H_n^{(2)'}(\Gamma_s a) \right] = -P_0\frac{n}{a}\varepsilon_n i^n J_n(\gamma_{c1}a)$$

$$-ik_z a A_n H_n^{(1)}(\gamma_{c1}a) - \left[(n+1)H_{n+1}^{(1)}(\gamma_{s1}a) + \gamma_{s1}a H_{n+1}^{(1)'}(\gamma_{s1}a)\right] B_n$$

$$-\omega k_z a \left[D_n H_n^{(1)}(\Gamma_c a) + E_n H_n^{(2)}(\Gamma_c a)\right] - i\omega \left\{ \left[(n+1)H_{n+1}^{(1)}(\Gamma_s a) + \Gamma_s a H_{n+1}^{(1)'}(\Gamma_s a)\right] F_n \right. \tag{41c}$$

$$\left. + \left[(n+1)H_{n+1}^{(2)}(\Gamma_s a) + \Gamma_s a H_{n+1}^{(2)'}(\Gamma_s a)\right] G_n \right\} = P_0 \varepsilon_n i^{n+1} k_z a J_n(\gamma_{c1}a)$$

$$\left[(i\omega\rho_1 - 2\mu_1 k_{c1}^2)H_n^{(1)}(\gamma_{c1}a) - 2\mu_1\gamma_{c1}^2 H_n^{(1)''}(\gamma_{c1}a)\right] A_n$$

$$+2i\mu_1 k_z \gamma_{s1} H_{n+1}^{(1)'}(\gamma_{s1}a)B_n - 2\frac{\mu_1 n}{a^2}\left[H_n^{(1)}(\gamma_{s1}a) - \gamma_{s1}a H_n^{(1)'}(\gamma_{s1}a)\right] C_n$$

$$- \left[2\mu_s^* \Gamma_{c1}^2 H_n^{(1)''}(\Gamma_c a) - \lambda^* K_c^{*2} H_n^{(1)}(\Gamma_c a)\right] D_n - \left[2\mu_s^* \Gamma_c^2 H_n^{(2)''}(\Gamma_c a) - \lambda^* K_c^{*2} H_n^{(2)}(\Gamma_c a)\right] E_n \tag{41d}$$

$$-2i\mu_s^* k_z \Gamma_s \left[F_n H_{n+1}^{(1)'}(\Gamma_s a) + G_n H_{n+1}^{(2)}(\Gamma_s a)\right]$$

$$+\frac{2\mu_s^* n}{a^2}\left\{\left[H_n^{(1)}(\Gamma_s a) - \Gamma_s a H_n^{(1)'}(\Gamma_s a)\right] K_n + \left[H_n^{(2)}(\Gamma_s a) - \Gamma_s a H_n^{(2)'}(\Gamma_s a)\right] L_n\right\}$$

$$= -P_0 \varepsilon_n i^n \left[(i\omega\rho_1 - 2\mu_1 k_{c1}^2)J_n(\gamma_{c1}a) - 2\mu_1\gamma_{c1}^2 J_n''(\gamma_{c1}a)\right]$$

$$-2\mu_1 n \left[H_n^{(1)}(\gamma_{c1}a) - a\gamma_{c1}H_n^{(1)'}(\gamma_{c1}a)\right] A_n - ik_z\mu_1 \left[(n+1)aH_{n+1}^{(1)}(\gamma_{s1}a) - \gamma_{s1}a^2 H_{n+1}^{(1)'}(\gamma_{s1}a)\right] B_n$$

$$-\mu_1 \left[n^2 H_n^{(1)}(\gamma_{s1}a) + \gamma_{s1}^2 a^2 H_n^{(1)''}(\gamma_{s1}a) - a\gamma_{s1}H_n^{(1)'}(\gamma_{s1}a)\right] C_n$$

$$-2\mu_s^* n \left\{\left[H_n^{(1)}(\Gamma_c a) - a\Gamma_c H_n^{(1)'}(\Gamma_c a)\right] D_n + \left[H_n^{(2)}(\Gamma_c a) - a\Gamma_c H_n^{(2)'}(\Gamma_c a)\right] E_n\right\}$$

$$+ik_z\mu_s^* \left\{\left[(n+1)aH_{n+1}^{(1)}(\Gamma_s a) - \Gamma_s a^2 H_{n+1}^{(1)'}(\Gamma_s a)\right] F_n \right. \tag{41e}$$

$$\left. + \left[(n+1)aH_{n+1}^{(2)}(\Gamma_s a) - \Gamma_s a^2 H_{n+1}^{(2)'}(\Gamma_s a)\right] G_n\right\}$$

$$+\mu_s^* \left[n^2 H_n^{(1)}(\Gamma_s a) + \Gamma_s^2 a^2 H_n^{(1)''}(\Gamma_s a) - a\Gamma_s H_n^{(1)'}(\Gamma_s a)\right] K_n$$

$$+\mu_s^* \left[n^2 H_n^{(2)}(\Gamma_s a) + \Gamma_s^2 a^2 H_n^{(2)''}(\Gamma_s a) - a\Gamma_s H_n^{(2)'}(\Gamma_s a)\right] L_n$$

$$= 2\mu_1 n P_0 \varepsilon_n i^n \left[J_n(\gamma_{c1}a) - aJ_n'(\gamma_{c1}a)\right]$$

$$-2ik_z\mu_1 a^2 \gamma_{c1} A_n H_n^{(1)'}(\gamma_{c1}a)$$

$$+\mu_1 \left\{\left[n+1-a^2 k_z^2\right] H_{n+1}^{(1)}(\gamma_{s1}a) - \gamma_{s1}a(n+1)H_{n+1}^{(1)'}(\gamma_{s1}a) - \gamma_{s1}^2 a^2 H_{n+1}^{(1)''}(\gamma_{s1}a)\right\} B_n$$

$$+ik_z\mu_1 an C_n H_n^{(1)'}(\gamma_{s1}a) - 2ik_z\mu_{s1}^* a^2 \Gamma_c \left[D_n H_n^{(1)'}(\Gamma_c a) + E_n H_n^{(2)'}(\Gamma_c a)\right]$$

$$-\mu_s^* \left\{\left[n+1-a^2 k_z^2\right] H_{n+1}^{(1)}(\Gamma_s a) - \Gamma_s a(n+1)H_{n+1}^{(1)'}(\Gamma_s a) - \Gamma_s^2 a^2 H_{n+1}^{(1)''}(\Gamma_s a)\right\} F_n \tag{41f}$$

$$-\mu_s^* \left\{\left[n+1-a^2 k_z^2\right] H_{n+1}^{(2)}(\Gamma_s a) - \Gamma_s a(n+1)H_{n+1}^{(2)'}(\Gamma_s a) - \Gamma_s^2 a^2 H_{n+1}^{(2)''}(\Gamma_s a)\right\} G_n$$

$$-ik_z\mu_s^* an \left[K_n H_n^{(1)}(\Gamma_s a) + L_n H_n^{(2)}(\Gamma_s a)\right] = 2P_0 \mu_1 \varepsilon_n i^{n+1} k_z \gamma_{c1} a^2 J_n'(\gamma_{c1}a)$$

Table 1
Parameter values used in calculations

Parameter	Gylcerine	Olive oil
μ (g/cm.s)	9.50	0.933
μ_b (g/cm.s)	9.50	0.933
c (cm/s)	1.91×10^5	1.44×10^5
ρ (g/cm^3)	1.25	0.9

$$i\omega\Gamma_c \left[D_n H_n^{(1)'}(\Gamma_c b) + E_n H_n^{(2)'}(\Gamma_c b) \right] - \omega k_z \left[F_n H_{n+1}^{(1)}(\Gamma_s b) + G_n H_{n+1}^{(2)}(\Gamma_s b) \right]$$

$$+ i\omega \frac{n}{b} \left[K_n H_n^{(1)}(\Gamma_s b) + L_n H_n^{(2)}(\Gamma_s b) \right] - \gamma_{c2} M_n J_n'(\gamma_{c2} b) + i k_z N_n J_{n+1}(\gamma_{s2} b) \tag{41g}$$

$$+ \frac{n}{b} Q_n J_n(\gamma_{s2} b) = 0$$

$$-i\omega \frac{n}{b} \left[D_n H_n^{(1)}(\Gamma_c b) + E_n H_n^{(2)}(\Gamma_c b) \right] - \omega k_z \left[F_n H_{n+1}^{(1)}(\Gamma_s b) + G_n H_{n+1}^{(2)}(\Gamma_s b) \right]$$

$$-i\omega\Gamma_s \left[K_n H_n^{(1)'}(\Gamma_s b) + L_n H_n^{(2)'}(\Gamma_s b) \right] + \frac{n}{b} M_n J_n(\gamma_{c2} b) + i k_z N_n J_{n+1}(\gamma_{s2} b) \tag{41h}$$

$$-\gamma_{s2} Q_n J_n'(\gamma_{s2} b) = 0$$

$$-k_z \omega b \left[D_n H_n^{(1)}(\Gamma_c b) + E_n H_n^{(2)}(\Gamma_c b) \right]$$

$$-i\omega \left[(n+1) H_{n+1}^{(1)}(\Gamma_s b) + \Gamma_s b H_{n+1}^{(1)'}(\Gamma_s b) \right] F_n - i\omega \left[(n+1) H_{n+1}^{(2)}(\Gamma_s b) + \Gamma_s b H_{n+1}^{(2)'}(\Gamma_s b) \right] G_n \tag{41i}$$

$$-i k_z b M_n J_n(\gamma_{c2} b) - \left[(n+1) J_{n+1}(\gamma_{s2} b) + \gamma_{s2} b J_{n+1}'(\gamma_{s2} b) \right] N_n = 0$$

$$\left[-\lambda^* K_c^{*2} H_n^{(1)}(\Gamma_c b) + 2\mu_s^* \Gamma_c^2 H_n^{(1)''}(\Gamma_c b) \right] D_n + \left[-\lambda^* K_c^{*2} H_n^{(2)}(\Gamma_c b) + 2\mu_s^* \Gamma_c^{*2} H_n^{(2)''}(\Gamma_c b) \right] E_n$$

$$+ 2 i k_z \mu_s^* \Gamma_s \left[F_n H_{n+1}^{(1)'}(\Gamma_s b) + G_n H_{n+1}^{(2)'}(\Gamma_s b) \right]$$

$$- \frac{2\mu_s^* n}{b^2} \left\{ \left[H_n^{(1)}(\Gamma_s b) - b\Gamma_s H_n^{(1)'}(\Gamma_s b) \right] K_n + \left[H_n^{(2)}(\Gamma_s b) - b\Gamma_s H_n^{(2)'}(\Gamma_s b) \right] L_n \right\} \tag{41j}$$

$$- \left[(i\omega\rho_2 - 2\mu_2 k_{c2}^2) J_n(\gamma_{c2} b) - 2\mu_2 \gamma_{c2}^2 J_n''(\gamma_{c2} b) \right] M_n$$

$$-2 i \mu_2 k_z \gamma_{s2} J_{n+1}'(\gamma_{s2} b) N_n + 2\mu_2 \frac{n}{b^2} \left[J_n(\gamma_{s2} b) - \gamma_{s2} b J_n'(\gamma_{s2} b) \right] Q_n = 0$$

$$2\mu_s^* n \left\{ \left[H_n^{(1)}(\Gamma_c b) - b\Gamma_c H_n^{(1)'}(\Gamma_c b) \right] D_n + \left[H_n^{(2)}(\Gamma_c b) - b\Gamma_c H_n^{(2)'}(\Gamma_c b) \right] E_n \right\}$$

$$- i k_z \mu_s^* \left\{ \left[(n+1) b H_{n+1}^{(1)}(\Gamma_s b) - \Gamma_s b^2 H_{n+1}^{(1)'}(\Gamma_s b) \right] F_n + \left[(n+1) b H_{n+1}^{(2)}(\Gamma_s b) - \Gamma_s b^2 H_{n+1}^{(2)'}(\Gamma_s b) \right] G_n \right\}$$

$$- \mu_s^* \left[n^2 H_n^{(1)}(\Gamma_s b) + \Gamma_s^2 b^2 H_n^{(1)''}(\Gamma_s b) - b\Gamma_s H_n^{(1)'}(\Gamma_s b) \right] K_n$$

$$- \mu_s^* \left[n^2 H_n^{(2)}(\Gamma_s b) + \Gamma_s^2 b^2 H_n^{(2)''}(\Gamma_s b) - b\Gamma_s H_n^{(2)'}(\Gamma_s b) \right] L_n \tag{41k}$$

$$+ 2\mu_2 n \left[J_n(\gamma_{c2} b) - b\gamma_{c2} J_n'(\gamma_{c2} b) \right] M_n + + i k_z \mu_2 \left[(n+1) b J_{n+1}(\gamma_{s2} b) - \gamma_{s2} b^2 J_{n+1}'(\Gamma_{s2} b) \right] N_n$$

$$+ \mu_2 \left[n^2 J_n(\gamma_{s2} b) + \gamma_{s2}^2 b^2 J_n''(\gamma_{s2} b) - b\gamma_{s2} J_n'(\gamma_{s2} b) \right] Q_n = 0$$

Table 2
Havriliak-Negami fitting parameters [40]

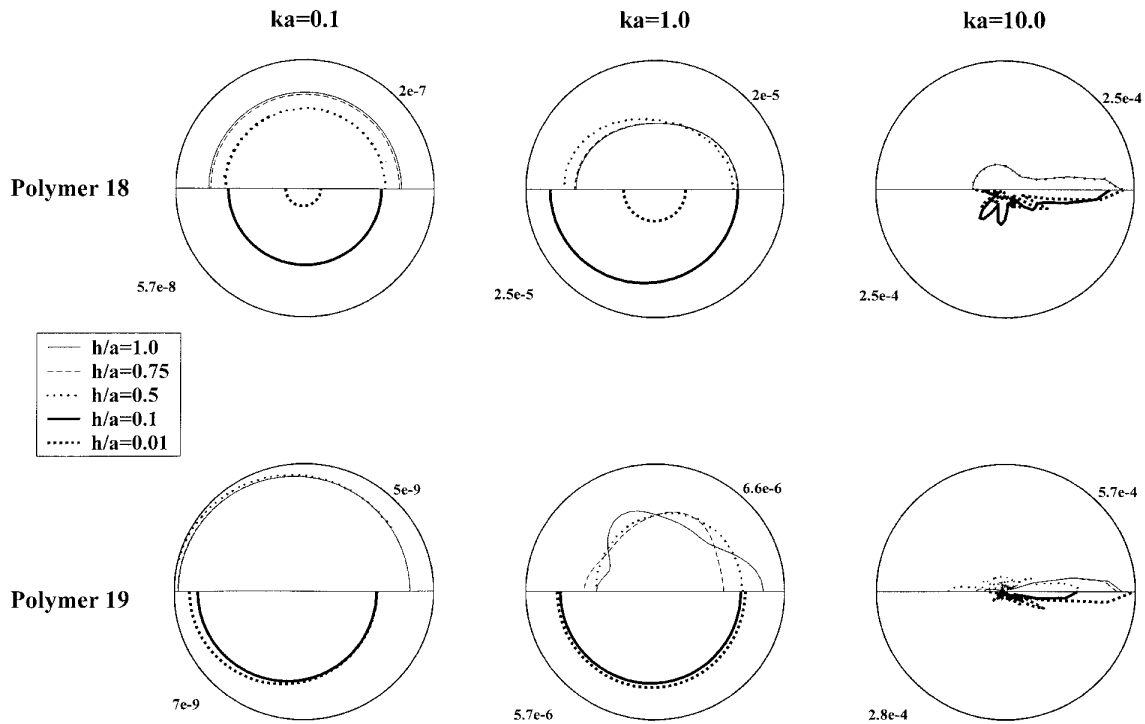|	Polymer 18	Polymer 19
G_0 (dynes/cm^2)	3.372 e7	5.019 e7
G_∞ (dynes/cm^2)	1.453 e10	0.8089 e10
τ (sec)	3.139 e-9	1.702 e-1
α	0.4822	0.4941
β	0.4116	0.1356
ρ_s (g/cm^3)	1.101	1.096
ν	0.5	0.5

Fig. 2. Angular distribution of the scattered far-field pressure for a unit amplitude plane wave incident upon an olive oil-filled spherical viscoelastic shell immersed in glycerine for selected dimensionless wave numbers and shell thicknesses.

$$2ik_z\mu_s^*b^2\Gamma_c\left[D_nH_n^{(1)'}(\Gamma_cb) + E_nH_n^{(2)'}(\Gamma_cb)\right]$$

$$+\mu_s^*\left\{\left[n+1-b^2k_z^2\right]H_{n+1}^{(1)}(\Gamma_sb) - \Gamma_sb(n+1)H_{n+1}^{(1)'}(\Gamma_sb) - \Gamma_s^2b^2H_{n+1}^{(1)''}(\Gamma_sb)\right\}F_n$$

$$+\mu_s^*\left\{\left[n+1-b^2k_z^2\right]H_{n+1}^{(2)}(\Gamma_sb) - \Gamma_sb(n+1)H_{n+1}^{(2)'}(\Gamma_sb) - \Gamma_s^2b^2H_{n+1}^{(2)''}(\Gamma_sb)\right\}G_n$$

$$+ik_z\mu_s^*bn\left[K_nH_n^{(1)}(\Gamma_sb) + L_nH_n^{(2)}(\Gamma_sb)\right] \tag{41l}$$

$$+2ik_z\mu_2b^2\gamma_{c2}M_nJ_n'(\gamma_{c2}b)$$

$$-\mu_2\left\{\left[n+1-b^2k_z^2\right]J_{n+1}(\gamma_{s2}b) - \gamma_{s2}b(n+1)J_{n+1}'(\gamma_{s2}b) - \gamma_{s2}^2b^2J_{n+1}''(\gamma_{s2}b)\right\}N_n$$

$$-ik_z\mu_2bnQ_nJ_n(\gamma_{s2}b) = 0$$

where $n = 0, 1, 2, \ldots$, except for Eqs (41b), (41e), (41h), (41k) where $n = 1, 2, \ldots$

Substitution of first of Eq. (33) into first of Eq. (24) yields the acoustic pressure for harmonic scattered waves. The radial component of the acoustic power flux vector (acoustic intensity) transmitted into the encapsulated fluid
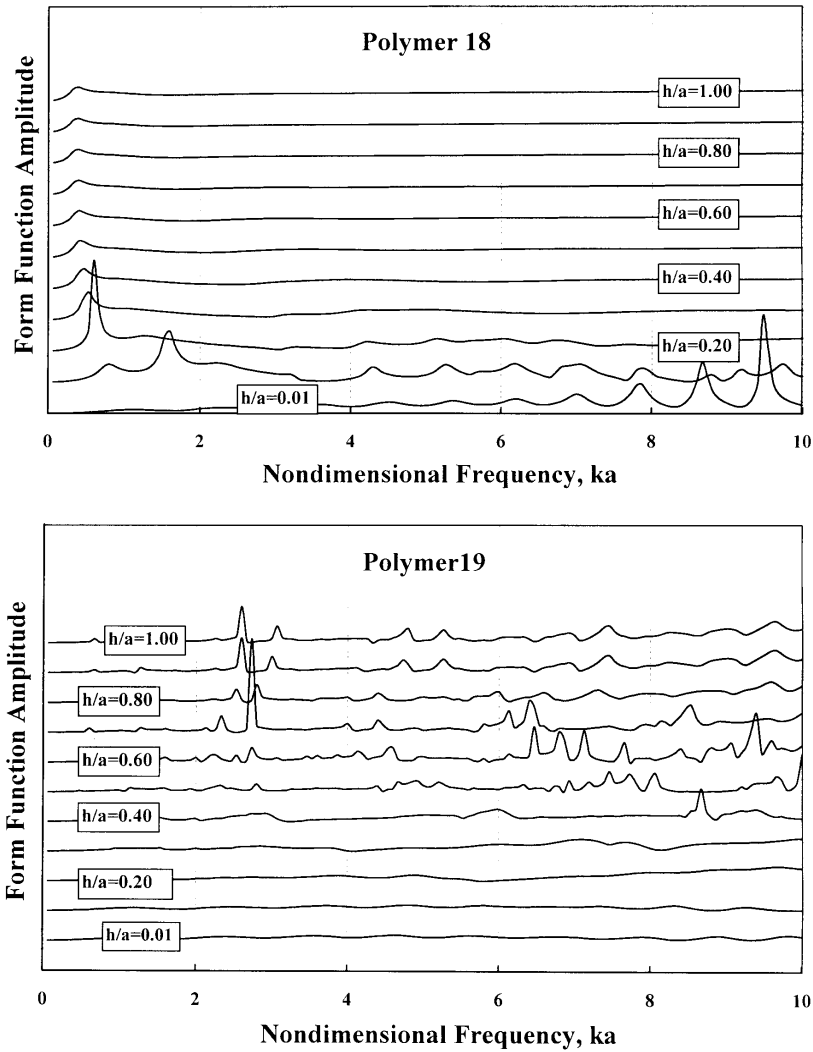
Fig. 3. Variation of the form function for the fluid-filled spherical viscoelastic shell with changes in shell thickness.

medium II per unit shell length may be obtained from [21]

$$I_{trans.}(r, \theta, z, \omega) = \frac{1}{2} Re \left\{ \sigma_{rr}^2 \times conj(u_r^2) + \sigma_{r\theta}^2 \times conj(u_\theta^2) + \sigma_{rz}^2 \times conj(u_z^2) \right\} \tag{42}$$

where $conj$ stands for the complex conjugate operator. Furthermore, since the incident wave is being propagated in an oblique direction with respect to the shell, the resultant force (per unit length) acting on the shell will therefore have two components that are given by [29,31]

$$F_x = a \int_0^{2\pi} (\sigma_{rr}^1 \cos\theta - \sigma_{r\theta}^1 \sin\theta) d\theta, \quad F_z = a \int_0^{2\pi} \sigma_{rz}^1 d\theta \tag{43}$$

in which the fluid stress tensor components as obtained from Eq. (38) may be expressed in the form

$$\sigma_{rr}^1 = \sum_{n=0}^{\infty} \sigma_{rrn}^1 \cos n\theta e^{ik_z z}$$

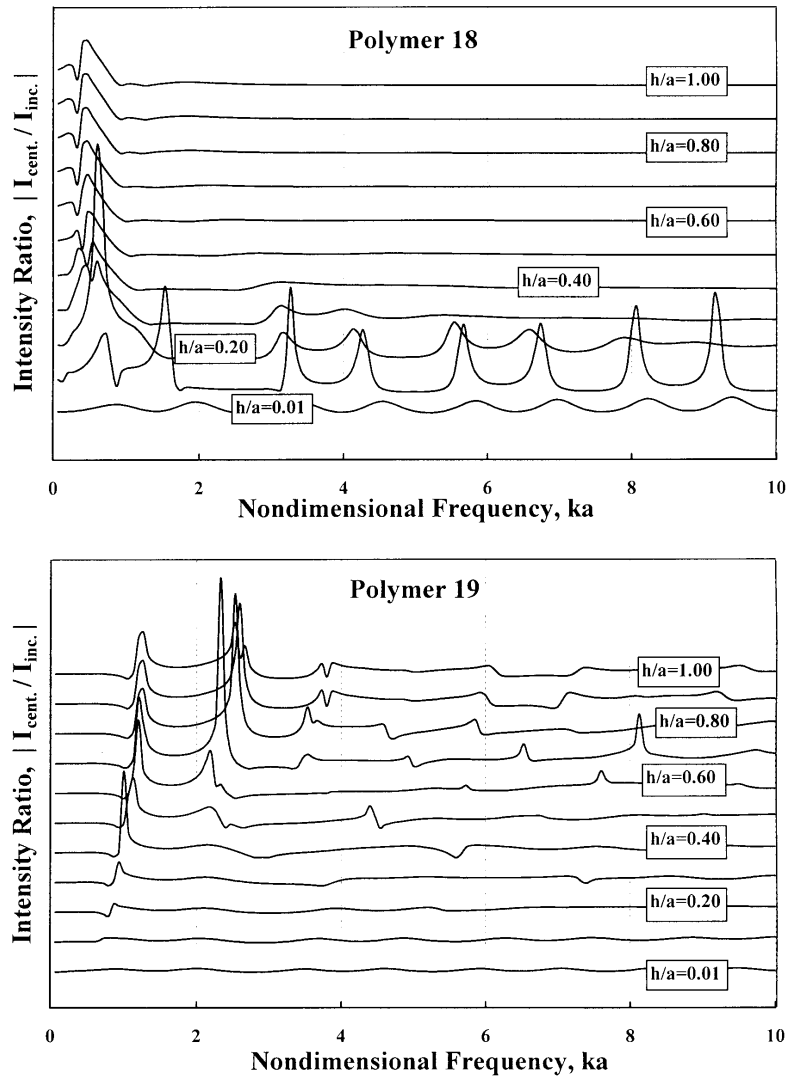$$\sigma_{r\theta}^1 = \sum_{n=1}^{\infty} \sigma_{r\theta n}^1 \sin n\theta e^{ik_z z} \tag{44}$$

Fig. 4. Variation of Transmitted acoustic intensity per unit incident wave intensity at the center of the fluid-filled spherical viscoelastic shell with the shell thickness.

$$\sigma_{rz}^1 = \sum_{n=0}^{\infty} \sigma_{rzn}^1 \cos n\theta e^{ik_z z}$$

Substituting the above expressions for the stress components into the force Eq. (43) and performing the integration, we find

$$F = \sqrt{F_x^2 + F_z^2} = \sqrt{\left[\pi\alpha(\sigma_{rr1}^1 - \sigma_{r\theta1}^1)\right]^2 + \left[2\pi a\sigma_{rz0}^1\right]^2} \tag{45}$$

where the appropriate orthogonality relations for the transcendental functions are employed.

6. Numerical results and discussion

In order to illustrate the nature and general behaviour of the solution, we consider numerical examples in this section. Realizing the large number of parameters involved here, no attempt is made to exhaustively evaluate the
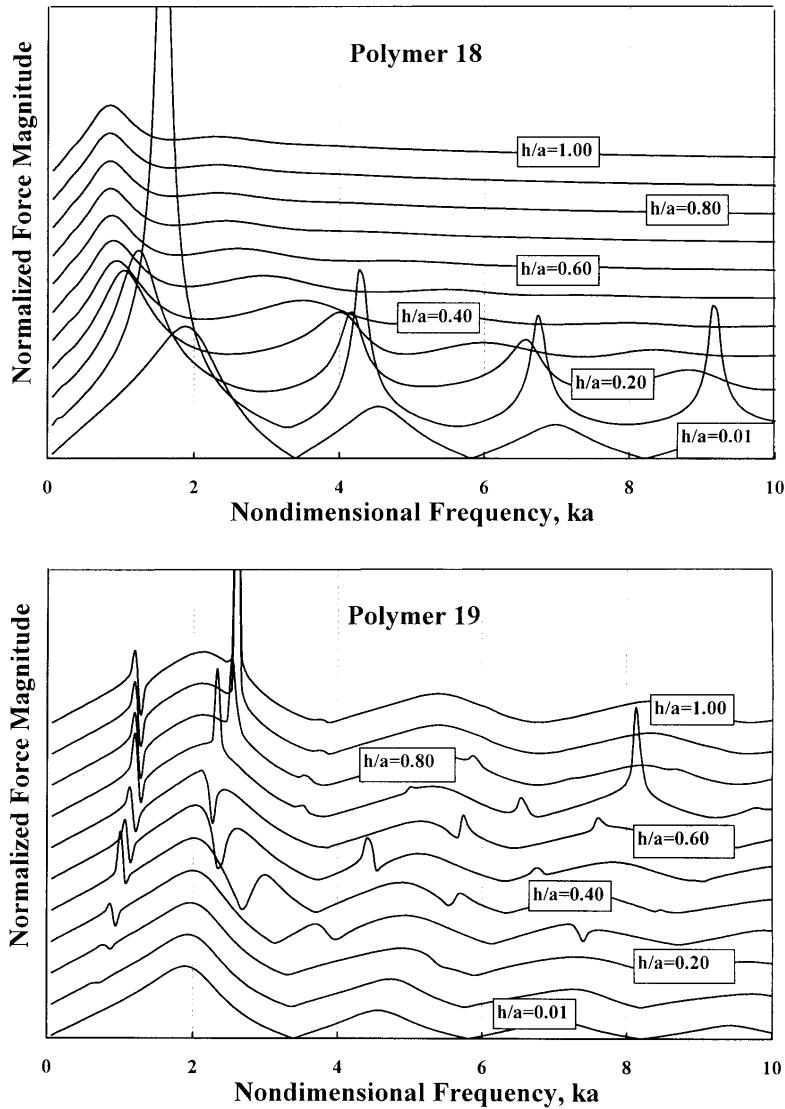
Fig. 5. Variation of the normalized acoustic force magnitude on the fluid-filled spherical viscoelastic shell with the shell thickness.

effect of varying each of them. The intent of the collection of data presented here is merely to illustrate the kinds of results to be expected from some representative and physically realistic choices of values for these parameters. From these data some trends are noted and general conclusions made about the relative importance of certain parameters. Noting the crowd of parameters that enter into the final expressions and keeping in view the availability of numerical data, we shall confine our attention to a particular model. The surrounding fluid is taken to be glycerine and the inner fluid is assumed to be olive oil with their assumed properties displayed in Table 1 [46]. As there are no reliable data found for the bulk viscosity of olive oil and glycerine, their numerical values are presumed to be equal to their shear viscosities. The viscoelastic shell material is supposed to be elastomeric with a fixed outer radius of $a = 0.05$ cm. Hartmann et al. [40], for the first time, reported all the input parameters necessary for a complete description of viscoelastic material properties for a set of (polyurethane) polymers within the context of Havriliak-Negami theory. The HN fitting parameters for two selected polymers with distinctively different dynamic viscoelastic properties in the frequency range of interest are compiled in Table 2. The corresponding fit of HN equations for shear modulus, $G'(\omega)$, and loss factor, $\eta(\omega)$, (e.g., Eqs (2) and (3)) for the selected polymers in a
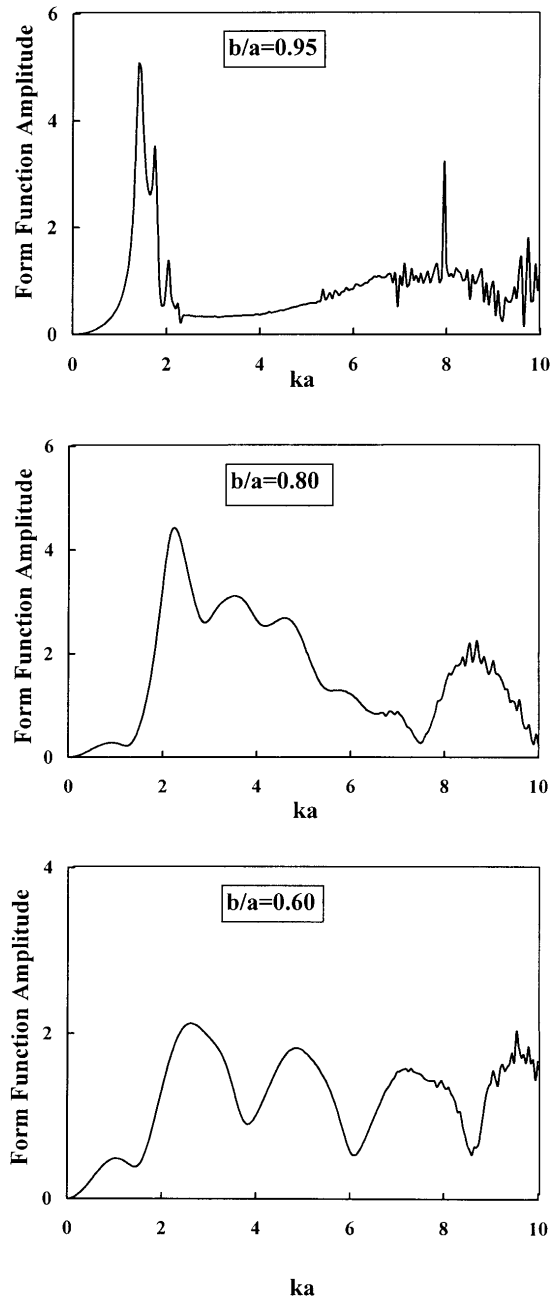
Fig. 6. Form function amplitude versus nondimensional frequency for a hollow duraluminium sphere immersed in water.

wide frequency range, are displayed in Figs 2a and 2b of [34], respectively. Polymer 18 is found to have the highest damping (loss factor), and polymer 19 is found to have the lowest damping in the frequency range of our interest (i.e., in $0.1 < ka < 10$). Accurate computation of Bessel functions of complex argument is achieved using MATLAB specialized math functions "besselh" and "besselj". The derivatives of Bessel functions were calculated by utilizing (9.1.27), (10.1.19) and (10.1.22) in [45]. A MATLAB code was constructed for treating boundary conditions and to calculate the unknown scattering coefficients and relevant acoustic field quantities as functions of nondimensional frequency ka where $k = Re(k_{c1}) = \omega a/c_1$.

Figure 2 displays the angular distribution of the scattered far-field pressure for a unit amplitude plane wave
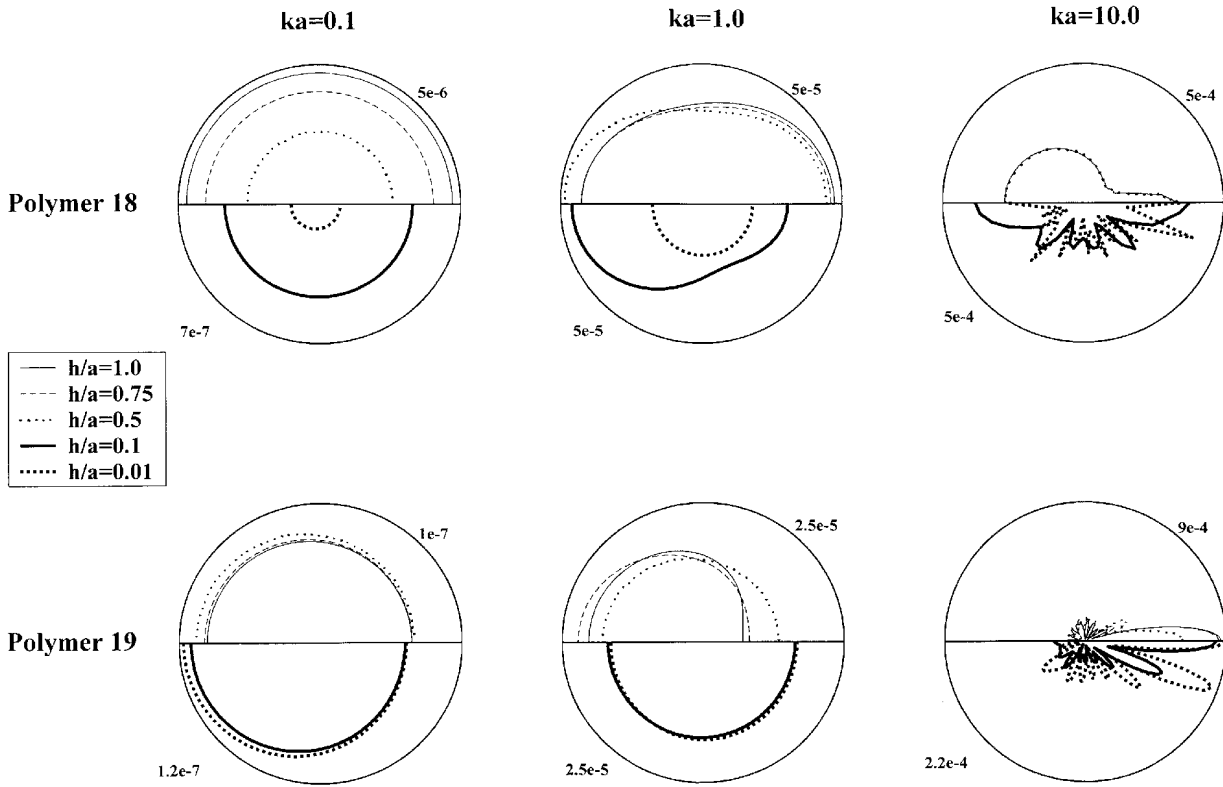
Fig. 7. Angular distribution of the scattered far-field pressure due to normal incidence of a unit amplitude plane wave on an olive oil-filled cylindrical viscoelastic shell immersed in glycerine for selected dimensionless wave numbers and shell thicknesses.

($P_0 = 1$.) incident upon an olive oil-filled spherical viscoelastic shell immersed in glycerine at selected dimensionless wave numbers and shell thicknesses. The far-field value of the radial coordinate in each case was simply chosen by making several computer runs while seeking for the convergence of the scattered pressure directivity patterns. The choice of $r_\infty = 10a$ was found to be adequate for all cases. Furthermore, a maximum number of forty modes were included in all summations in order to assure convergence in the high frequencies. It is very interesting to notice the change in directionality of the scattered waves as the frequency is varied. As seen from the figure, at low and intermediate frequencies (i.e., at $ka = 0.1, 1$) the pressure patterns are very uniform and they show a very low directionality, especially for the polymeric shell 18 that has the highest loss factor. Furthermore, increasing shell thickness has no important effect on the general far-field pressure distribution at these frequencies. However, at $ka = 10$ pressure directionality for both cases dramatically amplifies, especially for polymeric coating 19 that has the lowest loss factor. Furthermore, adding to the thickness of the polymeric shell 18 leads to a noticeable reduction in pressure pattern directionality at this frequency.

Figure 3 displays the variation of the forward-scattered far-field pressure magnitude (i.e., $|p_{scat.}(r_\infty, \pi)/p_{inc.}|$, or the form function amplitude) with nondimensional frequency and shell thickness. Here the main observation for polymeric shell 18 is that as its thickness increases, resonances in the pressure curves begin to shift to lower frequencies. For $h/a > 0.2$ there are almost no resonances in the intermediate and high frequencies and only a small peak is observed at $ka \approx 0.5$. For the polymeric shell 19, on the other hand, there are no resonances observed for $h/a < 0.4$. As the shell thickness increases beyond this critical value, relatively small amplitude resonances appear in the entire frequency range.

Figure 4 presents variations of the transmitted acoustic intensity (e.g., Eq. (28)) per unit incident wave intensity ($I_{inc.} = P_0^2 \rho \omega^2 / 2c$) at the center of the spherical shell with frequency and shell thickness. A similar trend as in the previous figure is evident. In particular, relatively high peaks for polymeric shell 18 (polymeric shell 19) at $h/a = 0.1, 0.2$ ($h/a \geqslant 0.7$) are observed. The change in normalized acoustic force magnitude (i.e., $|F|/\pi \rho \omega a^2 P_0$)
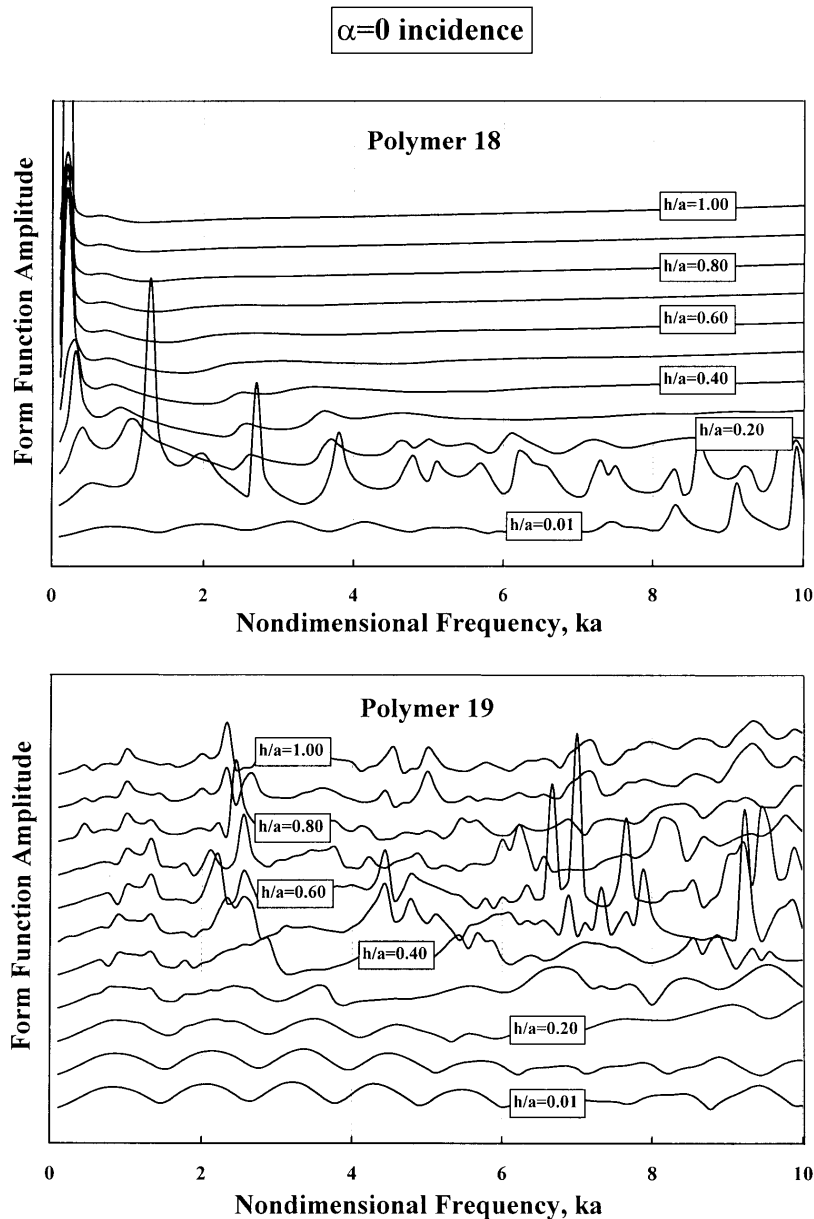
Fig. 8. Variation of the form function for the fluid-filled cylindrical viscoelastic shell with the shell thickness at normal wave incidence ($\alpha = 0$).

acting on the viscoelastic spherical shell with nondimensional frequency of the incident wave and shell thickness are presented in Fig. 5. The results are plotted in dimensionless form; namely, they are the acoustic radiation force per unit area and per unit pressure of the incident wave for the spherical shell. Once again, similar behaviour as in the previous two figures is observed. Here, the dimensionless force coefficients are almost linearly proportional to the dimensionless wave number ka when the frequency of the incident wave is low (i.e., $ka < 1$). The linearity breaks down when the incident wave frequency increases. Also, recurring peaks in the force amplitudes of the polymeric shell 18 are observed for $h/a \leqslant 0.4$. Adding to the thickness of polymeric shell 18 (i.e., $h/a > 0.5$) has in general no considerable effect on the force magnitudes as they become almost identical and non-oscillatory (i.e., there is only a single peak observed near $ka = 1$). A more regular pattern is noted for polymeric shell 19, especially at low shell thicknesses in the entire frequency range. This behaviour could be due to its lower loss factor and higher shear
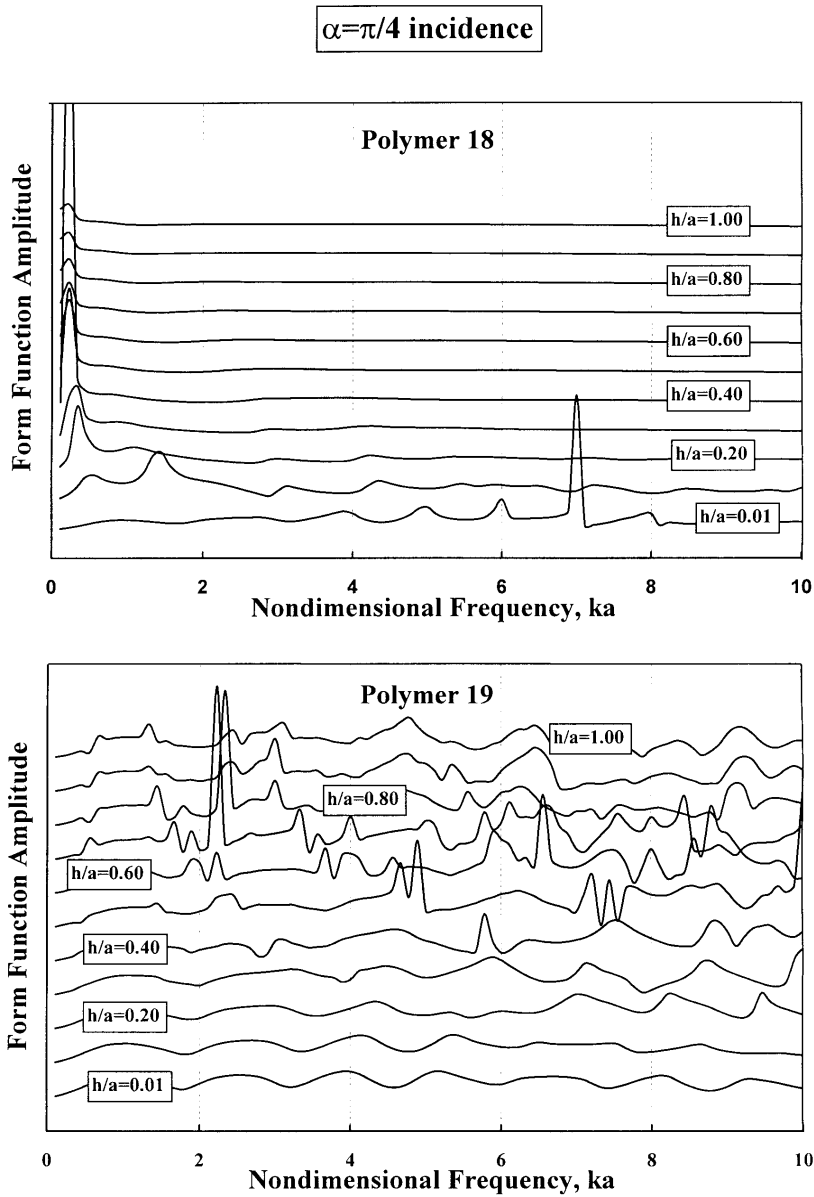
α=π/4 incidence

Fig. 9. Variation of the form function for the fluid-filled cylindrical viscoelastic shell with the shell thickness at oblique wave incidence ($\alpha = \pi/4$).

modulus in the frequency range of interest. Furthermore, a distinctively large peak in the force magnitude appears at $ka = 1.7$ and $h/a = 0.1$ ($ka = 2.6$ and $h/a > 0.9$) for polymeric shell 18 (polymeric shell 19). Moreover, as the incident wave frequency is increased, the force coefficient amplitudes gradually decrease for both polymeric shells. Lastly, in order to check overall validity of the first part of the work we computed the form function versus nondimensional frequency for a hollow duraluminium sphere immersed in water. The numerical results are shown in Fig. 6 that closely follow the curves displayed in Fig. 3 of [47]. The relatively small differences are mainly due to the inclusion of fluid viscosity in the current formulation.

Figure 7 displays the angular distribution of the scattered far-field pressure due to normal incidence ($\alpha = 0$) of a unit amplitude plane wave on an olive oil-filled cylindrical viscoelastic shell immersed in glycerine at selected dimensionless wave numbers and shell thicknesses. Here, observations analogous to the previous case can be made. Just as in the spherical shell situation, the patterns are very uniform in the low and intermediate frequencies for both
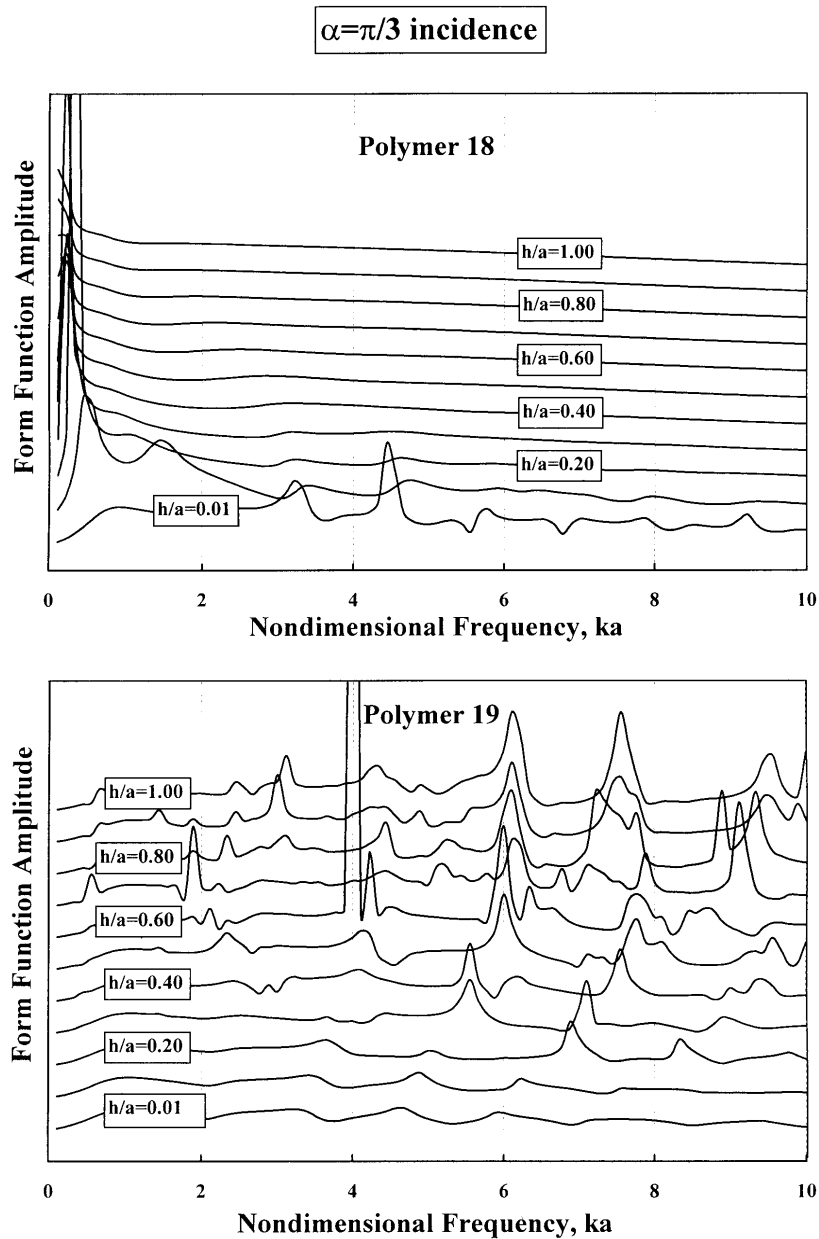
α=π/3 incidence

Fig. 10. Variation of the form function for the fluid-filled cylindrical viscoelastic shell with the shell thickness at oblique wave incidence ($\alpha = \pi/3$).

polymeric shells. However, at the high frequency of $ka = 10$, the pressure curves are much more directional with a relatively high forward scattering magnitude, especially for the polymeric shell 18.

Figures 8 through 10 display the variations of the forward-scattered far-field pressure magnitude (i.e., $|p_{scat.}(r_\infty, \pi)/p_{inc.}|$, or the form function amplitude) with nondimensional frequency and shell thickness for selected angles of wave incidence, i.e., $\alpha = 0, \pi/4, \pi/3$, respectively. Similar to the spherical shell case, the main observation for polymeric shell 18 is that as the shell thickness increases, resonances in the pressure curves begin to shift to lower frequencies. For this polymer, there are almost no resonances for $h/a > 0.2$ at the intermediate and high frequencies while a perceptible peak is observed at $ka \approx 0.2$. For the polymeric shell 19, on the other
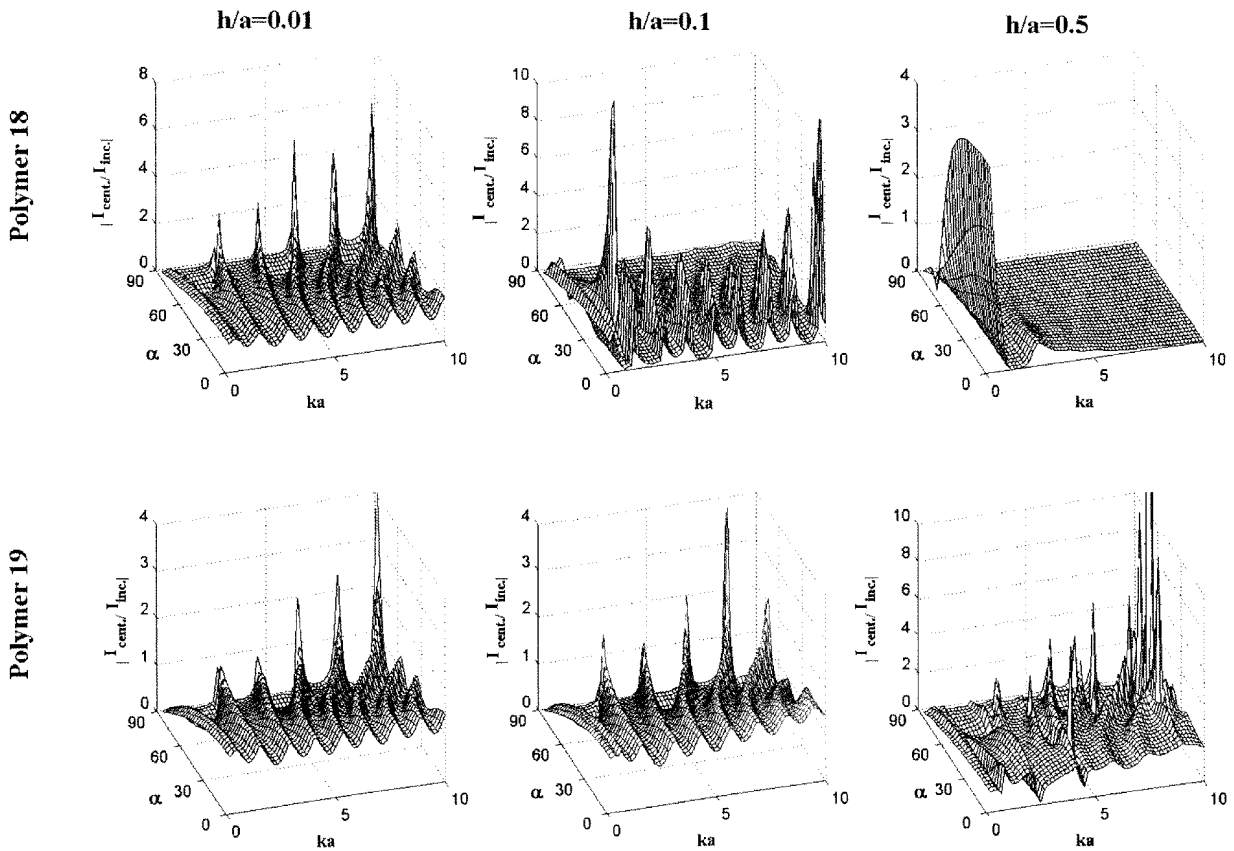
Fig. 11. Transmitted acoustic intensity at the center of the fluid-filled viscoelastic cylindrical shell per unit incident wave intensity versus nondimensional frequency and angle of wave incidence for selected shell thicknesses.

hand, relatively small magnitude resonances are observed for small shell thicknesses (i.e., $h/a < 0.4$). As the shell thickness is increased, the magnitude and number of these resonances increase in the entire frequency range of interest for all angles of wave incidence.

Figure 11 presents variations of the transmitted acoustic intensity (e.g., Eq. (42)) per unit incident wave intensity ($I_{inc.} = P_0\rho\omega^2/2c$) at the center of the cylindrical shell with nondimensional frequency and angle of wave incidence at selected shell thicknesses (i.e., $h/a = 0.01, 0.1, 0.5$). Here, we first observe that for $h/a = 0.01, 0.1$ the intensity ratio magnitudes display very regular and nearly harmonic surface patterns for both polymeric shells. In case of the very thick shell (i.e., $h/a = 0.5$), pattern oscillations decrease, especially for polymeric shell 18 that displays a relatively large peak at the low frequency of $ka \approx 0.8$ for $\alpha < \pi/3$. Furthermore, the surface patterns for the polymeric shell 19 become very irregular with the peaks occurring predominantly in the high frequency and large angle of incidence range.

Figure 12 displays the variations of normalized force magnitude (i.e., $|F|/2\pi\rho\omega aP_0$) acting on the cylindrical shells with respect to the nondimensional frequency and the angle of wave incidence for selected shell thicknesses. The results are plotted in dimensionless form; namely, they are the acoustic radiation force per unit area (per unit shell length). Here, we first note that the force magnitudes display regular, nearly harmonic and slightly damped surface patterns for both polymeric shells at $h/a = 0.01, 0.1$. In case of the thick polymeric shell 18 (i.e., $h/a = 0.5$), the overall force magnitude and the pattern oscillation level drastically decrease with nondimensional frequency. For the polymeric shell 19, the surface patterns turn out to be very irregular with relatively large peaks occurring predominantly in the high frequency and high angle of incidence range. Finally, in order to check overall validity of the second part of the work we computed the form function amplitude versus nondimensional frequency for a solid aluminium cylinder ($h/a \approx 1$) immersed in water at various angles of incidence. The numerical results are shown
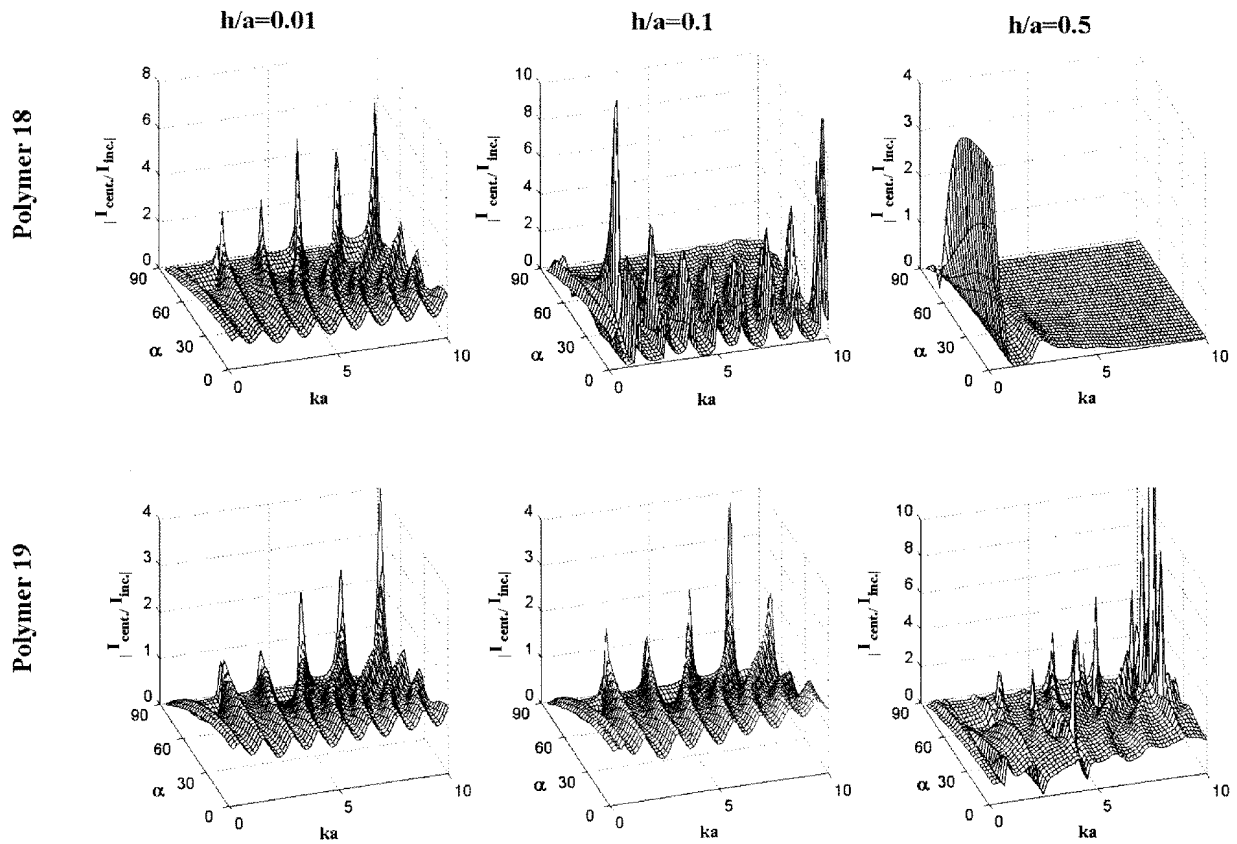
Fig. 12. Normalized force magnitude on the fluid-filled viscoelastic cylindrical shell versus nondimensional frequency and angle of wave incidence for selected shell thicknesses.

in Fig. 13 that closely follow the curves displayed in Fig. 2 of [48]. The small differences are mainly due to the inclusion of fluid viscosity in the current formulation.

7. Conclusion

This work presents analytical solutions as well as numerical results for two fundamental boundary value problems concerning the interaction of a plane sound wave with (viscous) fluid-loaded viscoelastic spherical and cylindrical shells filled with viscous fluids. The prime objective is to investigate the effects of dynamic viscoelastic shell material properties on acoustic scattering and its associated field quantities. Numerical results reveal the important consequences arising due to inclusion of Havriliak-Negami dynamic model for description of the viscoelastic material properties. The proposed model can lead to a better understanding of dynamic response of fluid-filled viscoelastic shells in an acoustic field. It may equally be useful in complementing the inverse scattering techniques that have been developed to determine the physical properties of viscoelastic materials from laboratory measurements of the scattered acoustic field [49].
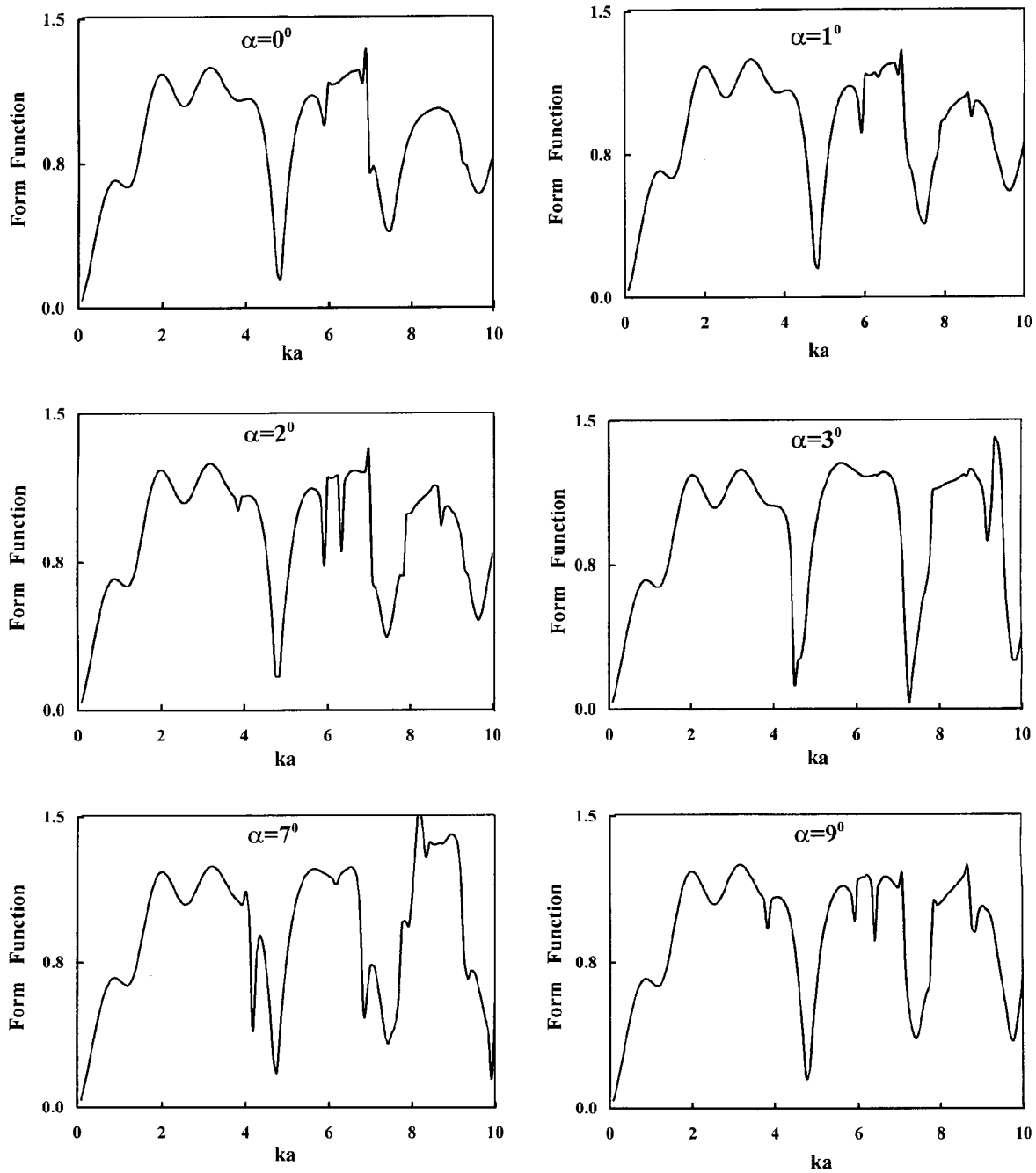
Fig. 13. Form function amplitude versus nondimensional frequency for a solid aluminium cylinder ($h/a \approx 1$) immersed in water for selected angles of wave incidence.

References

[1]   Lord Rayleigh, *The Theory of Sound,* (Vol. II), Dover, New York, 1945.
[2]   Sir H. Lamb, *Hydrodynamics,* Dover, New York, 1945.
[3]   P.M. Morse, *Vibration and Sound,* McGraw-Hill, New York, 1948.
[4]   L.V. King, On the Acoustic Radiation Pressure on Spheres, *Proc. Royal Soc. London Ser. A* **137** (1934), 212–240.

[5]   J.J. Faran, Sound Scattering by Solid Cylinders and Spheres, *J. Acoust. Soc. Am.* **23** (1951), 405–418.
[6]   T. Hasegawa, S. Kyosuke, I. Naoki and M. Kiichiro, Acoustic-Radiation Force Experienced by a Solid Cylinder in a Plane Progressive Sound Wave, *J. Acoust. Soc. Am.* **83** (1988), 1770–1775.
[7]   T.B. Li and M. Ueda, Sound Scattering of a Plane Wave Obliquely Incident on a Cylinder, *J. Acoust. Soc. Am.* **86** (1989), 2363–2370.
[8]   F. Honarvar and A.N. Sinclair, Scattering of an Obliquely Incident Plane Wave from a Circular Clad Rod, *J. Acoust. Soc. Am.* **102** (1997), 41–48.
[9]   V.V. Varadan, Y. Ma, V.K. Varadan and A. Lakhtakia, Scattering of Waves by Spheres and Cylinders, in: *Field Representations and Introduction to Scattering,* V.V. Varadan, A. Lakhtakia and V.K. Varadan, North-Holland, Amesterdam, 1991, pp. 211–322.
[10] J.M. Conoir, P. Rembert and J.L. Izbicki, Scattering by Cylindrical Objects at Oblique Incidence, in: *Acoustic Interactions with Submerged Elastic Structures, Part I: Acoustic Scattering and Resonances,* A. Guran, J. Ripoche and F. Ziegler, World Scientific, New York, 1998, pp. 81–128.
[11] M.C. Junger, Sound Scattering by Thin Elastic Shells, *J. Acoust. Soc. Am.* **24** (1952), 366–373.
[12] R.R. Goodman and R. Stern, Reflection and Transmission of Sound by Elastic Cylindrical Shells, *J. Acoust. Soc. Am.* **34** (1962), 338–344.
[13] R. Hickling, Analysis of Echoes From a Hollow Metallic Cylinder in Water, *J. Acoust. Soc. Am.* **36** (1964), 1124–1137.
[14] R.D. Doolittle and H. Uberall, Sound Scattering by Elastic Cylindrical Shells, *J. Acoust. Soc. Am.* **39**(2) (1966), 272–281.
[15] T. Hasegawa, H. Yasutaka, A. Akio, N. Hideki and K. Massahiko, Acoustic-Radiation Pressure Acting on Spherical and Cylindrical Shells, *J. Acoust. Soc. Am.* **93** (1993), 154–160.
[16] G. Maze, F. Leon and N.D. Veksler, Scattering of an Obliquely Incident Plane Acoustic Wave by a Circular Cylindrical Shell. Experimental Results, *Acta Acustica.* **84**(1) (1998), 1–11.
[17] G. Maze, J. Ripoch and V. Porochovskii, Scattering of an Obliquely Incident Plane Acoustic Wave by a Circular Cylindrical Shell. Results of Computations, *Acta Acustica.* **82**(5) (1996), 689–697.
[18] G.C. Gaunaurd, Sonar Cross Section of a Coated Hollow Cylinder in Water, *J. Acoust. Soc. Am.* **61** (1977), 360–368.
[19] L. Flax and W.G. Neubauer, Acoustic Reflection from Layered Elastic Absorptive Cylinders, *J. Acoust. Soc. Am.* **61** (1977), 307–312.
[20] S.H. Ko, Erratum: acoustic wave scattering from a coated cylindrical shell, *J. Acoust. Soc. Am.* **103** (1998), 599–600.
[21] S. Temkin, *Elements of Acoustics,* Wiley, New York, 1981.
[22] A.A. Doinikov, Acoustic Radiation Force on a Spherical Particle in a Visous Heat-Conducting Fluid, I. General Formula, *J. Acoust. Soc. Am.* **101**(2) (1997), 713–721.
[23] S.D. Danilov and M.A. Mironov, Mean Force on a Small Sphere in Sound Field in a Viscous Fluid, *J. Acoust. Soc. Am.* **107**(1) (2000), 143–153.
[24] A.S. Dukhin, P.J. Goetz, T.H. Wines and P. Somasundaran, Acoustic and Electroacoustic Spectroscopy, *Colloids and Surfaces* **173** (2000), 127–158.
[25] S. Temkin, Attenuation and Dispersion of Sound in Dilute Suspensions of Spherical Particles, *J. Acoust. Soc. Am.* **108**(1) (2000), 126–146.
[26] C.J.T. Sewell, The Extinction of Sound in a Viscous Atmosphere by Small Obstacles of Cylindrical and Spherical Form, *Philo. Trans. R. Soc. London* **A210** (1910), 239–270.
[27] P.S. Epstein and J. Carhart, The Absorption of Sound in Suspensions and Emulsions, *J. Acoust. Soc. Am.* **25** (1953), 553–565.
[28] J.R. Allegra and S.A. Hawley, Attenuation of Sound in Suspensions and Emulsions: Theory and experiments, *J. Acoust. Soc. Am.* **51** (1972), 1545–1564.
[29] W.H. Lin and A.C. Raptis, Acoustic Scattering by Elastic Solid Cylinders and Spheres in Viscous Fluid, *J. Acoust. Soc. Am.* **73**(3) (1983), 736–748.
[30] W.H. Lin and A.C. Raptis, Thermoviscous Effects on Acoustic Scattering by Thermoelastic Solid Cylinders and Spheres in Viscous Fluid, *J. Acoust. Soc. Am.* **74**(5) (1983), 241–250.
[31] W.H. Lin and A.C. Raptis, Sound Scattering from a Thin Rod in a Viscous Medium, *J. Acoust. Soc. Am.* **79**(6) (1986), 1693–1700.
[32] L.W. Anson and R.C. Chivers, Ultrasonic Scattering from Spherical Shells Including Viscous and Thermal Effects, *J. Acoust. Soc. Am.* **93**(4) (1993), 1687–1699.
[33] T. Hasegawa and Y. Watanabe, Acoustic Radiation Pressure on an Absorbing Sphere, *J. Acoust. Soc. Am.* **63**(6) (1978), 1733–1737.
[34] S.M. Hasheminejad and B. Harsini, Effects of Dynamic Viscoelastic Properties on Acoustic Diffraction By a Solid Sphere Submerged in a Viscous Fluid, *Archives of Applied Mechanics* **72**(1) (2002), 697–712.
[35] R.L. Willis, L. Wu and Y.H. Berthelot, Determination of the Complex Young's and Shear Dynamic Moduli of Viscoelastic Materials, *J. Acoust. Soc. Am.* **109**(2) (2001), 1–11.
[36] M. Soula, T. Vinh, Y. Chevalier and T. Beda, Measurements of Isothermal Complex Moduli of Viscoelastic Materials Over a Large Range of Frequencies, *J. Sound Vib.* **205**(2) (1997), 167–184.
[37] M. Giovagnoni, On the Direct Measurement of The Dynamic Poisson's Ratio, *Mech. Mater* **17** (1994), 33–46.
[38] J. Jarzynski, Mechanisms of Sound Attenuation in Matrials, in: *Sound and Vibration Damping with Polymers,* R.D. Cosaro and L.H. Sperling, American Chemical Society, Washington, DC, 1990, pp. 167–207.
[39] S. Havriliak and S. Negami, A Complex Plane Aalysis of α-Dispersions in Some Polymer Systems, in: *Transitions and Relaxations in Polymers, J. Polymer Sci., Part C, No. 14,* R.F. Boyer, ed., Interscience, New York, 1966, pp. 99–117.
[40] B. Hartman, G.F. Lee and J.D. Lee, Loss Factor Height and Width Limits for Polymer Relaxations, *J. Acoust. Soc. Am.* **95**(1) (1994), 226–233.
[41] M. Hasheminejad and T.L. Geers, Modal Impedance for Two Sphere in a Thermovicous Fluid, *J. Acoust. Soc. Am.* **94**(4) (1993), 2205–2214,
[42] J. Vollmann and J. Dual, High-Resolution Analysis of the Complex Wave Spectrum in a Cylindrical Shell Containing a Viscoelastic Medium, Part I. Theory and Numerical Results, *J. Acoust. Soc. Am.* **102**(2) (1997), 896–908.
[43] J.D. Achenbach, *Wave Propagation in Elastic Solids,* North-Holland, New York, 1976.
[44] P.M. Morse and K.U. Ingard, *Theoretical Acoustics,* McGraw-Hill, New York, 1968.
[45] M. Abramovitz and I.A. Stegun, *Handbook of Mathematical Functions,* National Bureau of Standards, Washington, DC, 1964.

[46] N.B. Vargaftik, *Handbook of Physical Properties of Liquids and Gases,* Springer-Verlag, Berlin, 1983.

[47] K.J. Diercks and R. Hickling, Echoes From Hollow Aluminum Spheres in Water, *J. Acoust. Soc. Am.* **41**(2) (1967), 380–393.

[48] T. Li and M. Ueda, Sound Scattering of a Plane Wave Obliquely Incident on a cylinder, *J. Acoust. Soc. Am.* **86**(6) (1989), 2363–2366.

[49] J.C. Piquette, Determination of the Complex Dynamic Bulk Modulus of Elastomers by Inverse Scattering, *J. Acoust. Soc. Am.* **77**(5) (1985), 1665–1673.